

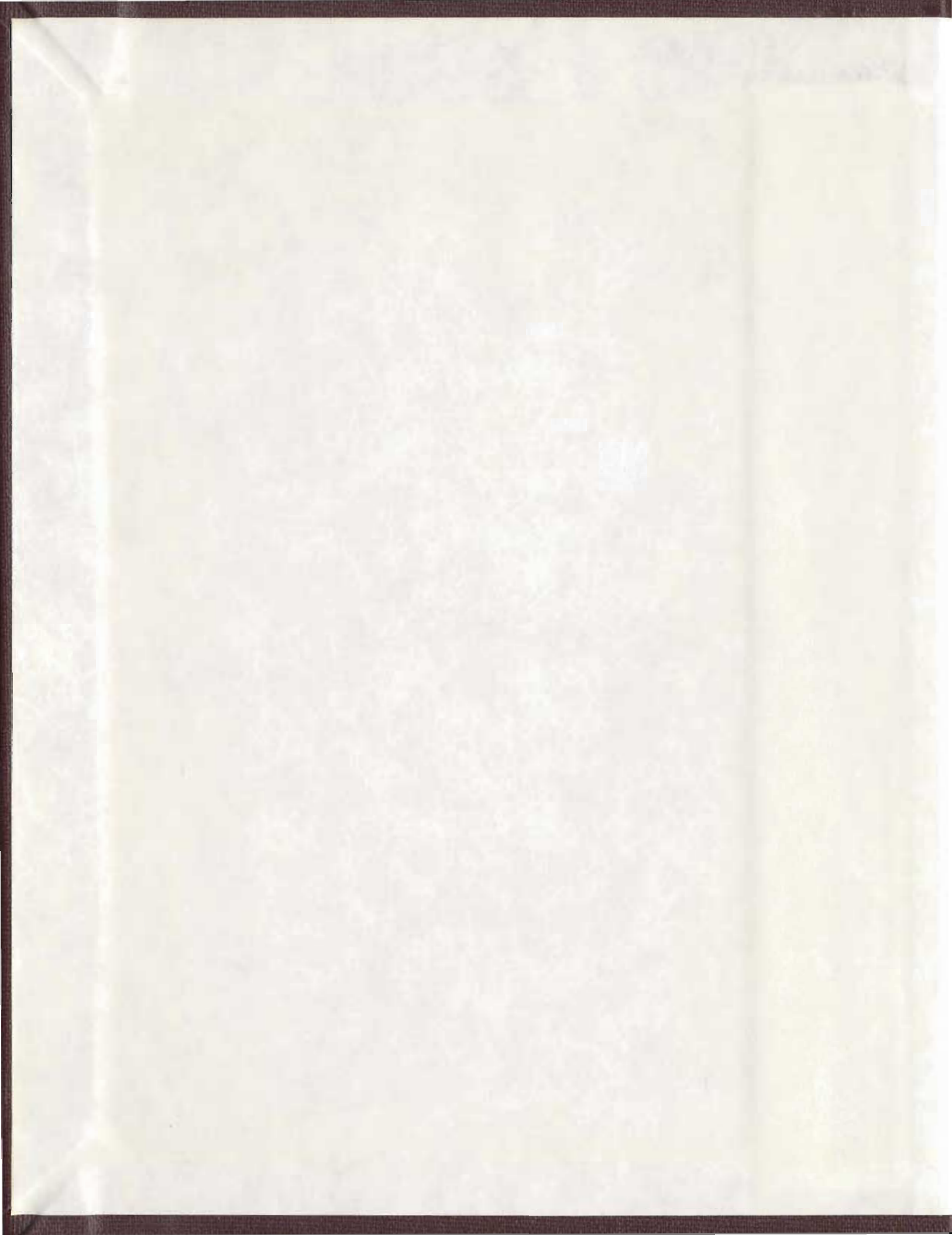
A STUDY OF SOME METAL  
COMPLEXES OF THE  
POLYDENTATE LIGAND 1,  
4-DI(2'-PYRIDYL)  
AMINOPHTHALAZINE

CENTRE FOR NEWFOUNDLAND STUDIES

TOTAL OF 10 PAGES ONLY  
MAY BE XEROXED

(Without Author's Permission)

JAMES ALFRED DOULL



100041





A STUDY OF SOME METAL COMPLEXES OF THE POLYDENTATE LIGAND

1,4-DI(2'-PYRIDYL)AMINOPHTHALAZINE

by

© James Alfred Doull, B.Sc.

A Thesis submitted in partial fulfillment of  
the requirement for the degree of  
Master of Science

Department of Chemistry  
Memorial University of Newfoundland

January 1979

St. John's

Newfoundland

## ABSTRACT

Coordination compounds of the ligand 1,4-di(2'-pyridyl)-aminophthalazine (PAP) and various nickel(II) and zinc(II) salts are studied. In the case of the nickel(II) complexes, infrared and electronic spectra, and elemental analyses indicate the compounds formed are binuclear and dimeric, containing nickel in a pseudo-octahedral environment; four of the coordination sites are occupied by ligand nitrogen atoms. In the nickel halide complexes the remaining coordination sites are occupied by water or, in some cases, coordinated halogen atoms, which are replaced by water in aqueous solution. Two complexes are formed with nickel nitrate, both of which contain coordinated nitrate groups, and one of them contains a bridging hydroxy group. In the coordination compounds of PAP with nickel perchlorate and tetrafluoroborate the metal atoms have coordinated water and are joined by a bridging hydroxy group. Magnetic susceptibility studies indicate antiferromagnetic exchange between the nickel atoms in the hydroxy bridged species.

When reacted with halides or pseudohalides of zinc, PAP acts in either a bidentate or tetradentate manner, depending on the anion present. All of the PAP-zinc complexes contain coordinated anions.

## ACKNOWLEDGEMENTS

I would like to express my gratitude to Dr. L.K. Thompson for his support and encouragement while this work was being carried out. Special thanks go to the Chemistry Department of The University of British Columbia for use of their magnetic balance, and to Dr. R.C. Thompson for his helpful discussions concerning the temperature dependent magnetic susceptibilities. I would also like to thank Dr. P. Golding for writing the computer program used for analysing the data from the magnetic studies. I am indebted to Dr. C. Jablonski for the time he spent carefully running NMR spectra, and for his assistance in interpreting them. I also thank Mrs. C. Chen for the skillful job she did in drafting the diagrams appearing in this work and Miss T. Barker for assistance in editing the work. Thanks also go to the Water Analysis Facility of the Chemistry Department of Memorial University of Newfoundland for their assistance in doing the metal analyses.

## TABLE OF CONTENTS

	Page
INTRODUCTION . . . . .	1
ELECTRONIC AND MAGNETIC PROPERTIES OF NICKEL(II) . . . . .	19
NICKEL(II) COMPLEXES OF PAP . . . . .	25
INFRARED SPECTRAL DATA . . . . .	26
NICKEL HALIDE COMPLEXES . . . . .	26
NICKEL NITRATE COMPLEXES . . . . .	26
NICKEL PERCHLORATE COMPLEX . . . . .	29
NICKEL TETRAFLUOROBORATE COMPLEX . . . . .	30
ELECTRONIC SPECTRA . . . . .	35
MAGNETIC MEASUREMENTS . . . . .	43
CONDUCTANCE DATA . . . . .	46
SUMMARY . . . . .	49
ZINC(II) COMPLEXES OF PAP . . . . .	55
INFRARED SPECTRAL DATA . . . . .	55
NUCLEAR MAGNETIC RESONANCE SPECTRAL DATA . . . . .	58
EXPERIMENTAL . . . . .	66
PREPARATIVE PROCEDURES . . . . .	69
PREPARATION OF THE LIGAND 1,4-DI(2'-PYRIDYL)AMINOPHTHALAZINE . . . . .	69
PREPARATION OF THE PAP-METAL COMPLEXES . . . . .	69
REFERENCES . . . . .	75
APPENDIX A . . . . .	77



## LIST OF TABLES

		Page
Table 1	Magnetic Parameters of Some PAP-Copper Complexes . . . . .	5
Table 2	Magnetic Moments and $\lambda_{MAX}$ Values for Some PAP-Nickel Complexes Prepared in Non-Aqueous Solvents . . . . .	8
Table 3	Magnetic Parameters of Some Nickel Complexes of DPPN, Me <sub>2</sub> DPPN and DHPH . . . . .	18
Table 4	Ligand and Water Vibrations of the PAP-Nickel Complexes . . . . .	32
Table 5	Anion Absorptions of PAP-Nickel Complexes . . . . .	33
Table 6	Vibrations of the (ClO <sub>4</sub> ) Group in Different Symmetry Environments . . . . .	34
Table 7	Electronic Spectral Data for the PAP-Nickel Complexes . . . . .	42
Table 8	Magnetic Parameters for the PAP-Nickel Complexes . . . . .	43
Table 9	Slopes of ( $\Lambda_o - \Lambda_e$ ) vs. $\sqrt{C_e}$ for Standard Ion Types in Water . . . . .	47
Table 10	Slopes of ( $\Lambda_o - \Lambda_e$ ) vs. $\sqrt{C_e}$ for PAP-Nickel Complexes in Aqueous Solutions . . . . .	47
Table 11	Infrared Spectral Data for Zinc Complexes of PAP . . . . .	57
Table 12	Chemical Shifts of the Protons of PAP and Some Zinc Complexes . . . . .	61
Table 13	Elemental Analyses of PAP-Zn Complexes . . . . .	74

## LIST OF FIGURES

		Page
Figure 1	Preparative Routes for PAP . . . . .	2
Figure 2	Tautomeric Forms of PAP . . . . .	3
Figure 3	The Structure of $[\text{PAPCu}_2\text{Cl}_3(\text{OH})]\cdot\text{H}_2\text{O}$ . . . . .	6
Figure 4	a) Structure of $[\text{M}_2(\text{PAA})_3]^{4+}$ . . . . .	10
	b) Octahedral Configuration of the Metal Atoms in $[\text{M}_2(\text{PAA})_3]^{4+}$ . . . . .	10
Figure 5	The Structures of DPPN, $\text{Me}_2\text{DPPN}$ , DPPLH And DHPH . . . . .	12
Figure 6	Proposed Structures of "Octahedral" $\text{trans-N}_4\text{O}_2$ And $\text{cis-N}_2\text{O}_4$ Binuclear Complexes . . . . .	14
Figure 7	Structure of the Cation $[\text{Ni}(\text{DHPH})(\text{H}_2\text{O})_2]_2^{4+}$ . . . . .	14
Figure 8	Proposed Structure for the Nickel(II) Complex of TAPH . . . . .	15
Figure 9	Proposed Structure for the Nickel(II) Complex of DAPH . . . . .	15
Figure 10	ORTEP Drawing of $[\text{Ni}_2(\text{DHPHTH})(\text{Cl})(\text{H}_2\text{O})_4]^{3+}$ . . . . .	17
Figure 11	Crystal Field Splitting Diagrams for Nickel(II) Ions in Various Crystal Fields . . . . .	20
Figure 12	Triplet Terms Arising from Nickel(II) Ions in Octahedral Fields . . . . .	22
Figure 13	Triplet Terms Arising from Nickel(II) Ions in Tetrahedral Fields . . . . .	22
Figure 14	A Comparison of the Electronic Spectrum of $[\text{Ni}(\text{H}_2\text{O})_6]^{2+}(\text{aq})$ with that of $[\text{PAP}_2\text{Ni}_2(\text{H}_2\text{O})_4]\text{Cl}_4(\text{aq})$ . . . . .	38
Figure 15	Effects of the Addition of conc. HCl on $\nu_1$ of $[\text{PAP}_2\text{Ni}_2(\text{H}_2\text{O})_4]\text{Br}_4(\text{aq})$ . . . . .	39

## LIST OF FIGURES

	Page
Figure 16	A Proposed Structure for the Cation in the Complex $[\text{PAP}_2\text{Ni}_2(\text{H}_2\text{O})_4]\text{Cl}_4$ . . . . . 53
Figure 17	A Proposed Structure for the Cation in the Complex $[\text{PAP}_2\text{Ni}_2(\text{OH})(\text{H}_2\text{O})_2](\text{ClO}_4)_3$ . . . . . 54
Figure 18	NMR Spectrum of PAP in DMSO . . . . . 62
Figure 19	NMR Spectrum of PAP in DMSO with Trifluoroacetic Acid Added . . . . . 63
Figure 20	NMR Spectrum of PAP-Zinc Chloride Complex in DMSO . . . . . 64
Figure 21	NMR Spectrum of PAP-Zinc Bromide Complex in DMSO . . . . . 65
Figure 22	Diagram of the Magnetic Balance Used for Temperature Dependent Susceptibility Studies . . . . . 68

## INTRODUCTION

The title compound, 1,4-di(2'-pyridyl)aminophthalazine (PAP) was originally prepared by Lever<sup>1</sup> via ring expansion of 1,3-di(2'-pyridyl)-iminoisoindoline with hydrazine hydrate (Fig. 1). This original synthesis is quite lengthy, since the preparation of the "isoindoline" precursor requires two reaction steps. The procedure was simplified by Thompson<sup>2</sup>, who prepared the "pyridylisoindoline" directly by fusion at 250° of phthalonitrile and 2-aminopyridine in a 1:2 molar ratio (Fig. 1).

The structure of PAP allows it to have three tautomeric forms:

a) both hydrogens on the phthalazine nitrogens, b) both hydrogens on the exocyclic nitrogens, c) one hydrogen on a phthalazine nitrogen and one on an exocyclic nitrogen (Fig. 2).

Between 4000 and 3100  $\text{cm}^{-1}$ , the infrared spectrum of PAP exhibits two absorptions, one at 3260 and the other at 3180  $\text{cm}^{-1}$ ; both bands have been assigned to N-H stretching<sup>2</sup>. Based on a comparison of the infrared spectrum of PAP with that of phthalaz-1,4-dione, the absorption at 3180  $\text{cm}^{-1}$  was assigned to phthalazine N-H stretch. However, this absorption shows up in all of the PAP complexes of nickel, and does not shift when the complex is prepared from anhydrous nickel salts in  $\text{D}_2\text{O}$ . On the basis of these data, the absorption at 3180  $\text{cm}^{-1}$  has been reassigned to aromatic C-H stretch; the band at 3260  $\text{cm}^{-1}$  is assigned to N-H stretch, this absorption shifts to lower energy by 860  $\text{cm}^{-1}$  in complexes prepared from  $\text{D}_2\text{O}$ .

Although the infrared spectrum of PAP is complicated, it has been found that one of the pyridine ring absorptions is of diagnostic use in spectroscopic studies of PAP metal complexes. The infrared spectra of

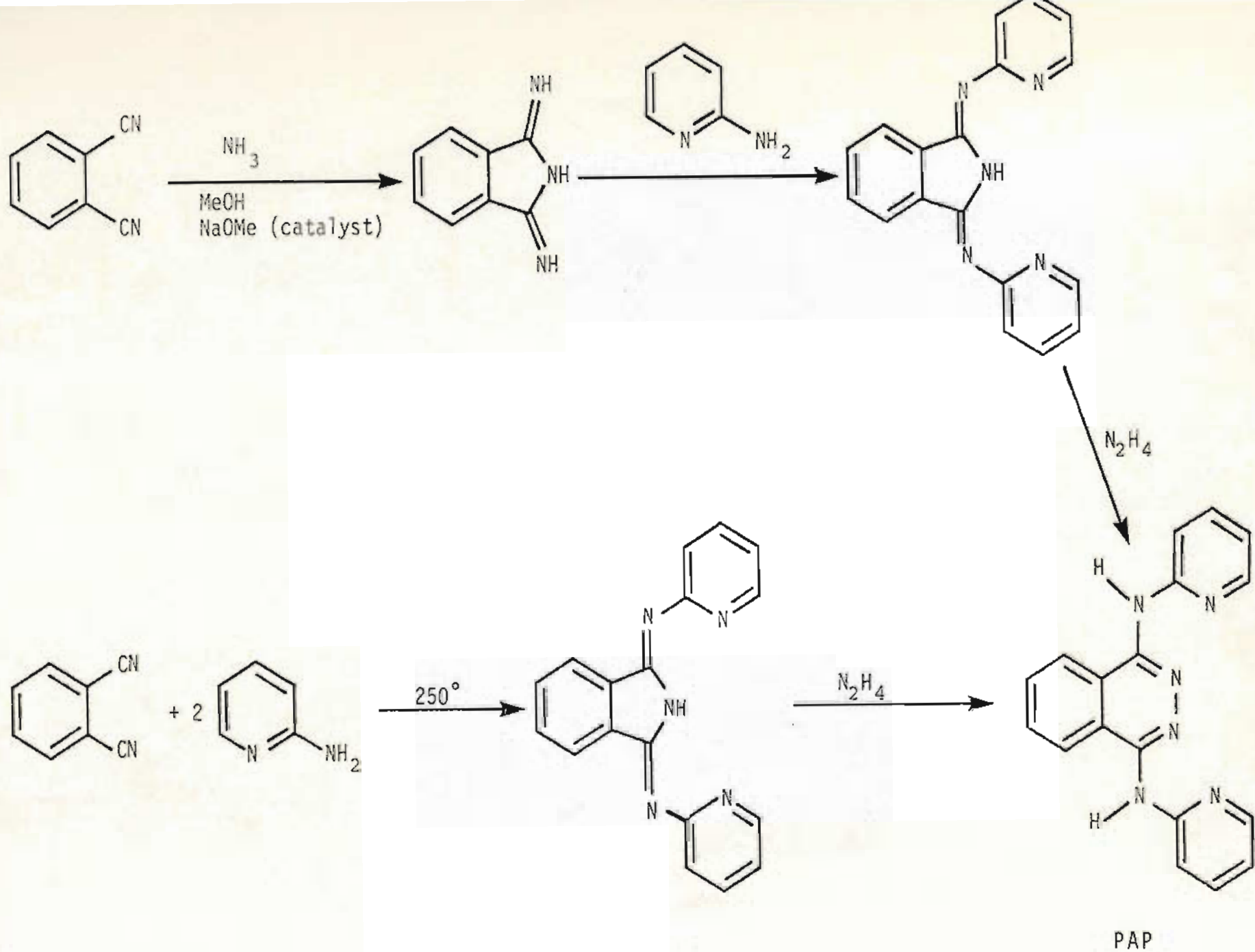
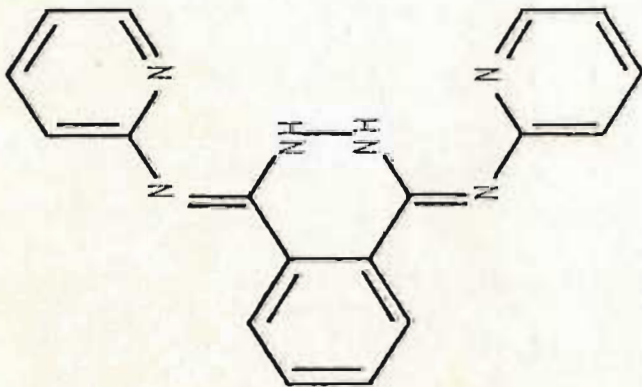
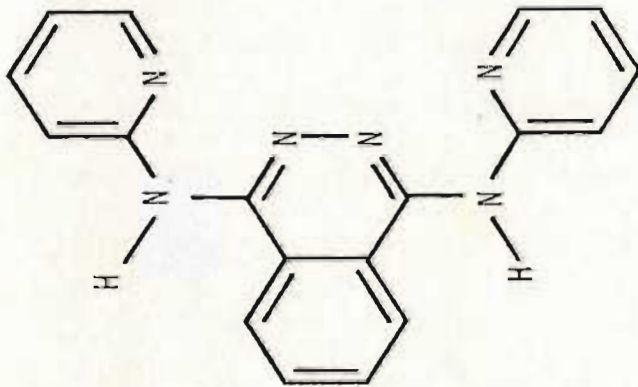


FIG. 1

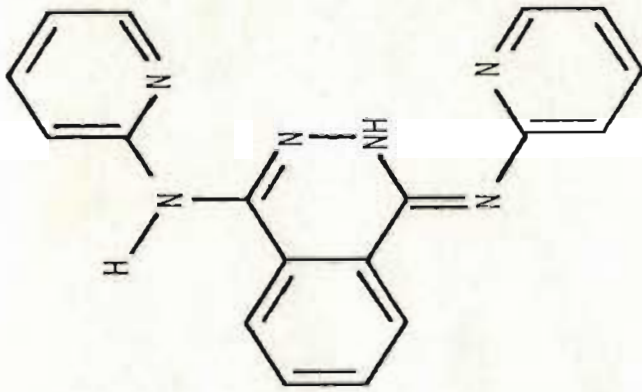
PREPARATIVE ROUTES FOR PAP



( a )



( b )



( c )

FIG. 2

TAUTOMERIC FORMS OF PAP

pyridine and substituted pyridines show no remarkable changes when the ring is coordinated to the metal atom, but a ring breathing mode absorption at  $990\text{ cm}^{-1}$  for the free pyridine does shift by  $30\text{-}40\text{ cm}^{-1}$  to higher energy on coordination<sup>3-6</sup>. For such complexes as  $\text{Cu}(\text{py})_2\text{Cl}_2$ ,  $\text{Cu}(\text{py})_2\text{Br}_2$  and  $\text{Co}(\text{py})_4(\text{NCS})_2$  the pyridine ring breathing mode absorption appears around  $1020\text{ cm}^{-1}$ . For 2-aminopyridine complexes, the band is observed to shift from  $983$  to  $1010\text{ cm}^{-1}$  on coordination.

The infrared spectrum of 1,4-diaminophthalazine shows no absorption between  $1010$  and  $950\text{ cm}^{-1}$ , but that of PAP shows a strong band at  $989\text{ cm}^{-1}$ , assigned to the ring breathing mode absorption of the uncoordinated pyridine rings. For bidentate complexes of PAP (i.e. coordination via one phthalazine nitrogen and one pyridine nitrogen), a shift in the ring breathing mode absorption is expected for only the coordinated ring, giving rise to two bands; if the ligand is tetradentate, there should be no ligand absorption at  $989\text{ cm}^{-1}$ .

PAP is known to react in a tetradentate fashion with salts of copper and cobalt, forming binuclear compounds in which each metal atom is coordinated to one phthalazine and one pyridine nitrogen atom<sup>7,8</sup>.

Binuclear complexes,  $\text{PAPCu}_2\text{X}_3(\text{OH})\cdot\text{H}_2\text{O}$  ( $\text{X} = \text{Cl}, \text{Br}$ ) may be prepared by direct reaction of the ligand with an aqueous solution of the appropriate copper salt; an iodate complex,  $\text{PAPCu}_2(\text{IO}_3)_3(\text{OH})\cdot 3\text{H}_2\text{O}$  is prepared by adding a saturated aqueous solution of potassium iodate to aqueous  $\text{PAPCu}_2\text{Cl}_3(\text{OH})\cdot\text{H}_2\text{O}$ <sup>7</sup>. A preliminary X-ray study of the chloride complex shows that each copper atom is five-coordinate in a square-pyramidal environment with the metal atoms joined by bridging chlorine

and hydroxy groups.<sup>9</sup> (Fig. 3). The room temperature magnetic moments of these complexes, as well as the values of the exchange integral, J, are given in Table 1.

TABLE 1  
MAGNETIC PARAMETERS OF SOME PAP-COPPER COMPLEXES

COMPLEX	$\mu_{\text{eff}}$ (B.M.) (295°K)	$\bar{g}$	-J (cm <sup>-1</sup> )	REF
PAPCu <sub>2</sub> Cl <sub>3</sub> (OH)·H <sub>2</sub> O	1.60	2.28	100	7
PAPCu <sub>2</sub> Br <sub>3</sub> (OH)·H <sub>2</sub> O	1.66	2.10	85	1
PAPCu <sub>2</sub> (IO <sub>3</sub> ) <sub>3</sub> (OH)·3H <sub>2</sub> O	1.34	1.95	167	1

The large values of J indicate an antiferromagnetic interaction between the copper atoms coordinated to the same ligand. In the case of the halide complexes, it is assumed that magnetic exchange takes place via the bridging groups. Haddad and Hendrickson<sup>10</sup> have reported a linear relationship between J and the Cu-(OH)-Cu bridge angle in certain dihydroxy bridged amine chelate compounds they have studied; the bridge angle for these complexes varied from 95.6° for [Cu(bipyridine)-(OH)]<sub>2</sub>(NO<sub>3</sub>)<sub>2</sub> to 104.8° for [Cu(TMEN)(OH)]<sub>2</sub>Br<sub>2</sub> (TMEN = N,N,N',N'-tetramethylethylenediamine). The mono-hydroxy bridged copper amine chelates such as [Cu<sub>2</sub>(TREN)<sub>2</sub>(OH)]X<sub>3</sub> (TREN = 2,2',2''-triaminotriethylamine; X = ClO<sub>4</sub>, PF<sub>6</sub>) have larger values of J, a consequence of the larger Cu-(OH)-Cu bridge angle in these systems. The larger value of J for the PAP-copper iodate complex when compared to those of the simple



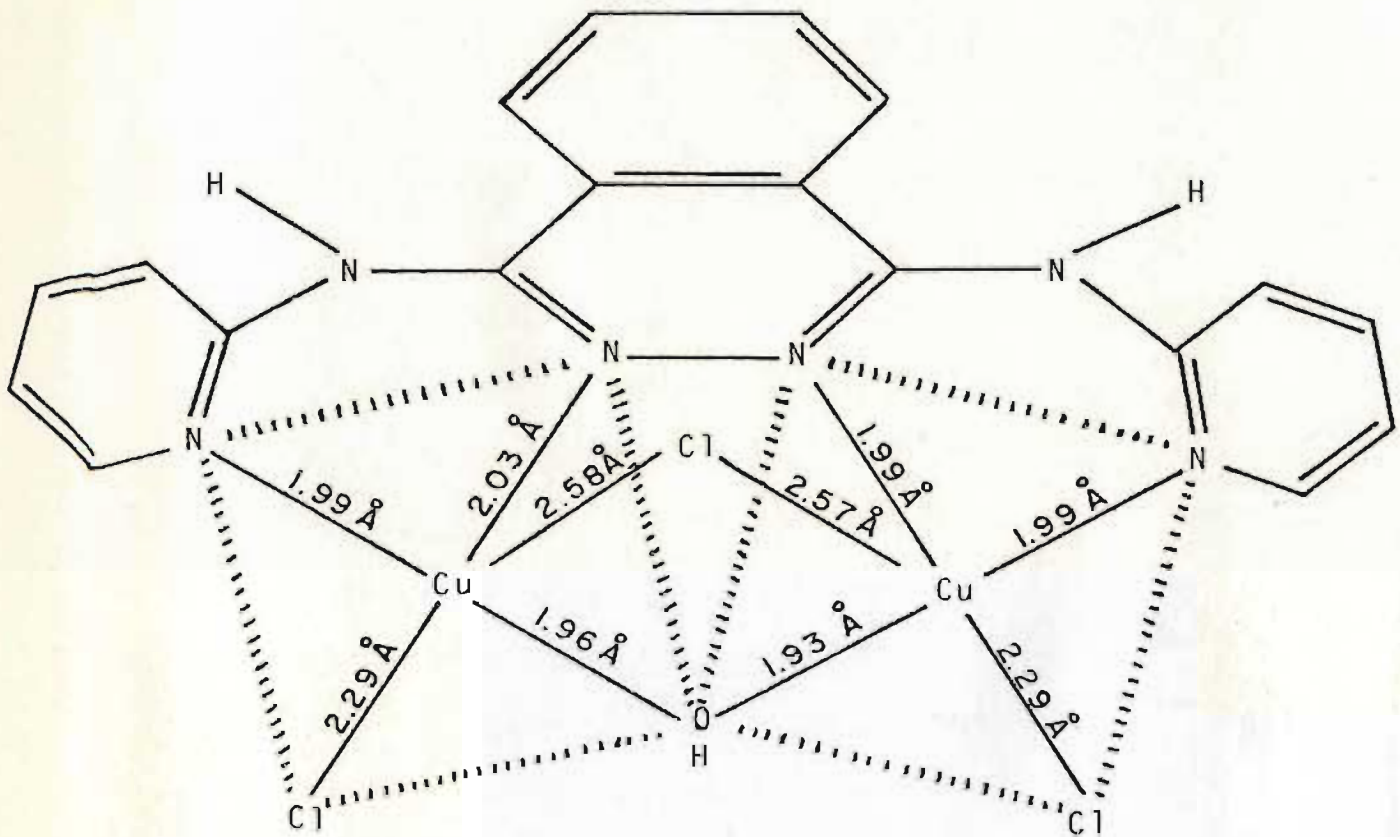


Fig.3

THE STRUCTURE OF  $[PAPCu_2Cl_3(OH)] \cdot (H_2O)$  AS INDICATED BY X-RAY CRYSTALLOGRAPHY<sup>9</sup>. THE WATER MOLECULE IS IN THE CRYSTAL LATTICE UNCOORDINATED TO THE COPPER ATOMS.

halide complexes may indicate a larger OH bridge angle, or if direct metal-metal exchange is involved, it may be a case of a shorter distance between the copper atoms, as has been postulated by Thompson et al.<sup>7</sup>

Two series of complexes were prepared by reaction of PAP with copper carboxylates:  $\text{PAPCu}_2(\text{RCO}_2)_3$  and  $\text{PAPCu}_2(\text{RCO}_2)_4$ .<sup>7</sup> The formula of the complex formed is apparently dependent on the  $\text{pK}_a$  of the corresponding carboxylic acid; if the  $\text{pK}_a$  is less than 3.8, a tetracarboxylate forms; if the  $\text{pK}_a$  is greater than this value, a tricarboxylate forms. It is assumed the ligand is anionic in the tricarboxylate forms and neutral in the tetracarboxylate complexes, suggesting the  $\text{pK}_a$  of the complexed ligand is around 3.8. Neither the halide nor the carboxylate complexes show an infrared absorption between 950 and 1010  $\text{cm}^{-1}$ , but an extra band is observed between 1010 and 1022  $\text{cm}^{-1}$ , indicating that both pyridine nitrogen atoms are coordinated.

Cobalt(II) halides in various solvents react with PAP in a 2:1 molar ratio to form compounds which analyse as  $\text{PAPCo}_2\text{X}_3$  ( $\text{X} = \text{Cl}, \text{Br}, \text{I}$ ).<sup>8</sup> Solvated forms are obtained from methanol and water, but convert to the unsolvated forms when vacuum dried. It is interesting to note that the chloride complex is thermochroic in methanol. At room temperature the solution is red, but when heated turns green. The green form is less soluble than the red form, green crystals being obtained when the solution is heated and the volume reduced. Electronic spectroscopic studies indicate the green form,  $\text{PAPCo}_2\text{Cl}_3$ , contains pseudo-tetrahedral cobalt. The red form has not been clearly characterised, but probably

contains octahedral cobalt(II). Recent evidence in our laboratory has shown that aqueous solutions of the binuclear cobalt complexes are oxygen sensitive, and diamagnetic binuclear cobalt(III) derivatives can be obtained.<sup>11</sup>

Preliminary studies on some nickel(II) complexes of PAP prepared in non-aqueous solvents have been carried out by Thompson<sup>2</sup>. These complexes, the solvent in which they were prepared, the  $\lambda_{\text{max}}$  values of the solid state electronic spectra, as well as the room temperature magnetic moments are summarised in Table 2.

TABLE 2  
MAGNETIC MOMENTS AND  $\lambda_{\text{MAX}}$  VALUES FOR SOME PAP-NICKEL COMPLEXES  
PREPARED IN NON-AQUEOUS SOLVENTS

COMPOUND	SOLVENT	$\mu_{\text{eff}}$ (B.M.)	$\lambda_{\text{MAX}}$ (cm <sup>-1</sup> )
PAPNi <sub>2</sub> Cl <sub>3</sub> ·4H <sub>2</sub> O	ACETIC ACID	3.08	10,000, 16,000 [30,000]
PAPNiBr <sub>2</sub> ·2H <sub>2</sub> O	ACETIC ACID	3.10	10,900, 17,000 [30,000]
PAPNiI <sub>2</sub> ·2H <sub>2</sub> O	METHANOL	3.11	7,700, 12,200 [25,000]
PAPNi <sub>2</sub> (NCS) <sub>2</sub> ·4H <sub>2</sub> O	METHANOL	2.96	9,800, 16,700 [30,000]

SOURCE: Reference 2, Table 17.

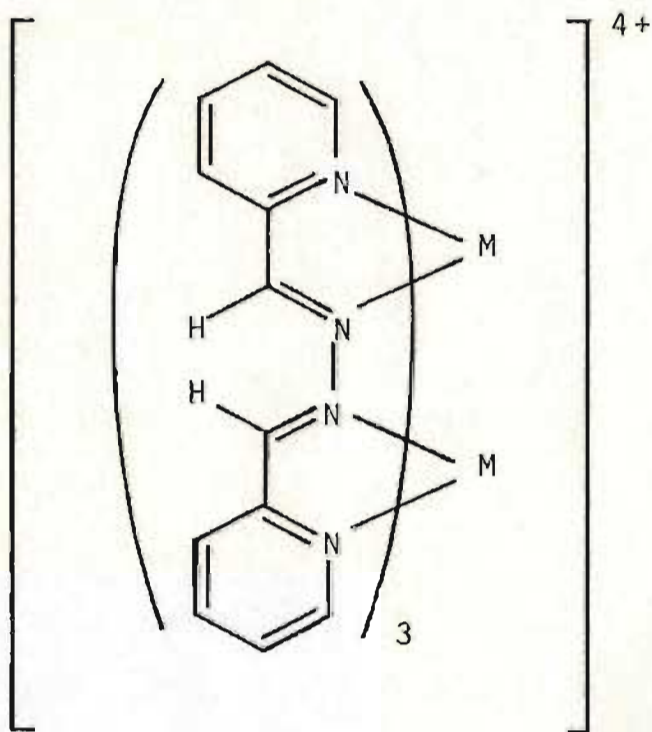
[ ] DENOTES APPROXIMATE POSITIONS OF HIGHEST ENERGY LIGAND-FIELD BANDS

The presence of two pyridine ring breathing mode absorptions in the infrared spectra of the bromide and iodide complexes indicates that these compounds are probably mononuclear. The electronic spectra are characteristic of octahedral nickel(II); the absence of noticeable splitting of  $\nu_1$  (see section on Electronic Spectra) indicates there is no strong tetragonal distortion of the coordination environment around the nickel atoms in the solid state.

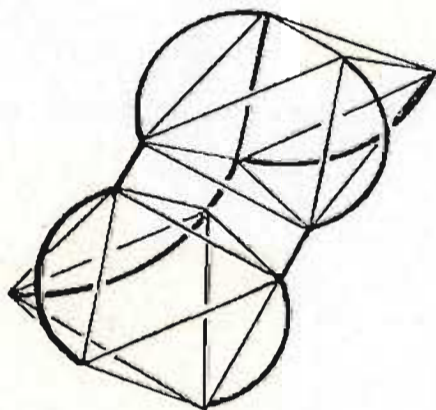
Ligands with a functional similarity to PAP (nitrogen atoms spaced similarly to the coordinating nitrogens of PAP) have been known since at least 1947, when Stratton and Busch<sup>12-14</sup> described iron(II) and nickel(II) complexes of 2-pyridinealdazine (PAA) e.g.  $[M(PAA)_2]X_2$  ( $M = Fe, Ni$ ;  $X = I, ClO_4, BF_4$ )<sup>13,14</sup>. In these systems PAA is tridentate, coordinated through the two pyridine and one of the azine nitrogens. If these reaction solutions are cooled rapidly from room temperature, compounds of empirical formula  $[M_2(PAA)_3]X_4$  form. These latter complexes are not stable in aqueous solution, and slowly dissociate to form  $[M(PAA)_3]^{2+}$  and  $M^{2+}$ .

Aqueous conductance measurements, magnetic susceptibilities and electronic spectra are consistent with a complex cation  $[M_2(PAA)_3]^{4+}$  containing two octahedrally coordinated metal atoms held adjacent to each other by three tetradentate ligands (Fig. 4). Molecular models indicate that such a structure is sterically feasible provided that each ligand is twisted approximately  $60^\circ$  about its N-N bond.

Ball and Blake have prepared a number of binuclear nickel(II)<sup>15</sup> and cobalt(II)<sup>16</sup> complexes of 3,6-di-(2'-pyridyl)pyridazine (DPPN),



(a)



(b)

FIG. 4

a). STRUCTURE OF  $[M_2(PAA)_3]^{4+}$

b). OCTAHEDRAL CONFIGURATION OF THE METAL ATOMS IN  $[M_2(PAA)_3]^{4+}$ . SHADED LINES REPRESENT LIGAND MOLECULES. METAL ATOMS ARE IN CENTRES OF OCTAHEDRA (NOT SHOWN).

3,6-di-(6-methylpyrid-2-yl)pyridazine ( $\text{Me}_2\text{DPPN}$ ), 3,5-di-(2'-pyridyl)pyrazole (DPPLH), and 1,4-dihydrazinophthalazine (DHPH) (Fig. 5).

The grey-green nickel complexes of DPPN,  $\text{Ni}(\text{DPPN})(\text{NO}_3)_2 \cdot 2\text{H}_2\text{O}$  and  $\text{Ni}(\text{DPPN})(\text{ClO}_4)_2 \cdot 2\text{H}_2\text{O}$  have four bands in their electronic spectra at about 10,000, 12,000, 17,000, and 18,000  $\text{cm}^{-1}$ , and also strong absorption above 22,000  $\text{cm}^{-1}$ . These four bands are interpreted as representing the electronic transitions of tetragonally distorted octahedral nickel(II). The electronic spectra of the green complexes  $\text{Ni}_2(\text{DPPN})(\text{SO}_4)_2 \cdot 5\text{H}_2\text{O}$  and  $\text{Ni}_2(\text{Me}_2\text{DPPN})(\text{NO}_3)_4 \cdot 2\text{H}_2\text{O}$  show only two absorptions below 22,000  $\text{cm}^{-1}$ , one around 10,000 and the other around 16,700  $\text{cm}^{-1}$ . These transitions are more typical of regular octahedral nickel(II). The greater splitting of the octahedral energy levels in the complexes with a 1:1 metal:ligand ratio compared to those with a 2:1 ratio is attributed to the ligand atoms in the case of the former being arranged as "trans"- $\text{N}_4\text{O}_2$ ; the latter are probably "cis"- $\text{N}_2\text{O}_4$ . Probable structures for these binuclear dimeric ("trans"- $\text{N}_4\text{O}_2$ ) and binuclear monomeric ("cis"- $\text{N}_2\text{O}_4$ ) complexes are shown in Fig. 6. A structure such as that proposed in Fig. 6a might suggest steric strain because of the proximity of the hydrogen atoms at the "6" positions of the pyridine rings; however, molecular models indicate that this interference can be relieved by slight distortion. A much more severe strain would be experienced by 1:1 complexes of  $\text{Me}_2\text{DPPN}$ , and this ligand only produces 1:2 and 2:1 (metal:ligand) complexes.

The infrared spectra of the nitrate complexes suggest the anions are coordinated. In the 1:1 complexes, e.g.  $\text{Ni}(\text{DPPN})(\text{NO}_3)_2 \cdot \text{H}_2\text{O}$ , the nitrate groups act in a unidentate manner. The anion absorptions

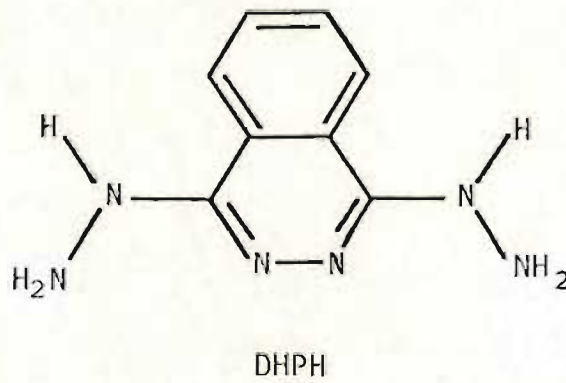
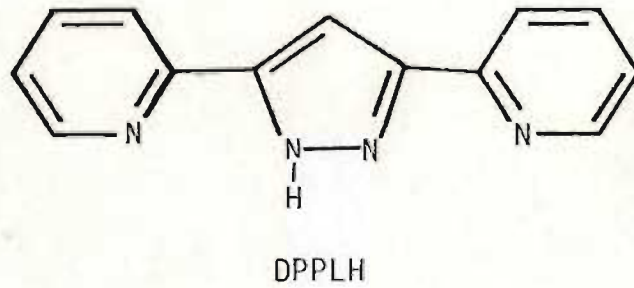
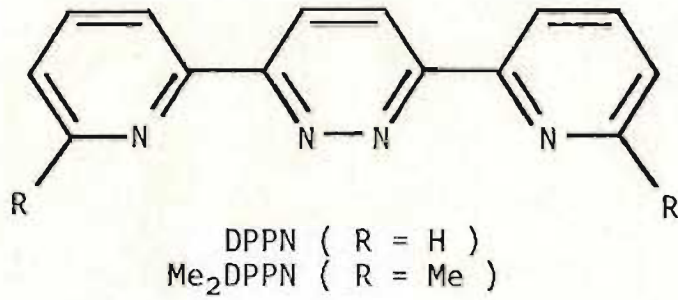


FIG. 5

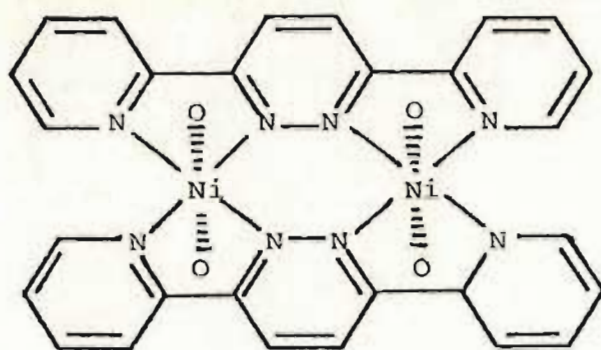
in the spectra of the 2:1 complexes e.g.  $\text{Ni}_2(\text{Me}_2\text{DPPN})(\text{NO}_3)_4 \cdot 2\text{H}_2\text{O}$  suggest the presence of both uni- and bidentate nitrate groups.

The purple or grey complexes  $\text{Ni}(\text{DHPH})(\text{H}_2\text{O})_2\text{X}_2 \cdot 3\text{H}_2\text{O}$  ( $\text{X} = \text{Cl}, \text{Br}, \text{I}$ ) all have similar electronic spectra, consisting of three bands at approximately 9,400, 13,500, and 18,800  $\text{cm}^{-1}$  (no absorptions above 18,800  $\text{cm}^{-1}$  are reported). The central band is split into two components, about 700  $\text{cm}^{-1}$  apart, which are poorly resolved, even at low temperature. The spectrum is interpreted in terms of the octahedral  ${}^3\text{T}_{2g}$  and  ${}^3\text{T}_{1g}$  levels being split by 4,000 - 5,000  $\text{cm}^{-1}$  in a tetragonal field such that two of the resulting four levels almost coincide. An X-ray structural determination of the dimeric complex  $\text{Ni}(\text{DHPH})\text{Cl}_2 \cdot 3\text{H}_2\text{O}$  reveals the cation to be centrosymmetric, with the nickel atoms in a tetragonally distorted octahedral environment<sup>17</sup> (Fig. 7).

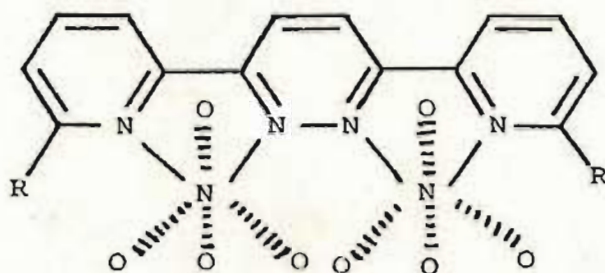
The magnetic moments,  $g$ , and  $J$  values of the DPPN,  $\text{Me}_2\text{DPPN}$  and DHPH complexes are quoted in Table 3. As may be seen from the table, all of these complexes are paramagnetic, having magnetic moments ranging from ca. 2.8 - 2.9 B.M. The  $J$  values indicate spin-spin interaction between the nickel atoms, which is thought to occur through the azine nitrogen bridge of the ligand.

Two complexes prepared by Rosen<sup>18</sup> contain two nickel atoms circumscribed by the macrocyclic ligands 6,7,8,9,12,19,20,21,22, 25-decahydro-8,8,10,21,21,23-hexamethyl-5,26:13,18-bis(azo)-dibenz[i,t][1,2,6,7,12,13,17,18]-octaazacyclodocosine (TAPH) and 4-[2-(4-hydrazino-1-phthalazinyl)-hydrazino]-4-methyl-2-pentanone-((4-hydrazino-1-phthalazinyl)hydrazone) (DAPH) (see Figs. 8, 9).





( a )



( b )

FIG. 6

PROPOSED STRUCTURES OF "OCTAHEDRAL"  
TRANS- $N_4O_2$  (a), AND CIS- $N_2O_4$  (b) COMPLEXES

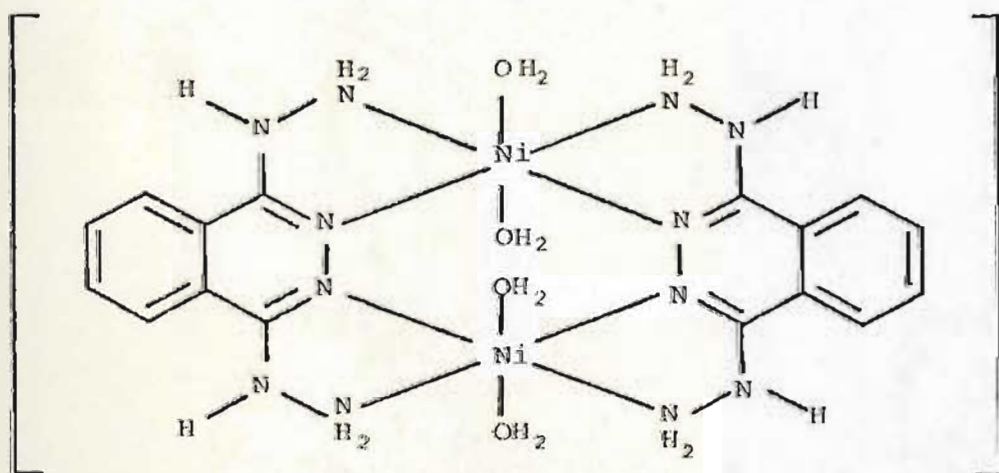


FIG. 7

STRUCTURE OF THE CATION  $[Ni(DHPH)(H_2O)_2]_2^{4+}$   
AS INDICATED BY X-RAY ANALYSIS, (Ni-N = 2.07-2.10Å ;  
Ni-O = 2.16Å ; Ni-Ni = 3.79Å ;  $\angle$  Ni-N-N = 125° )

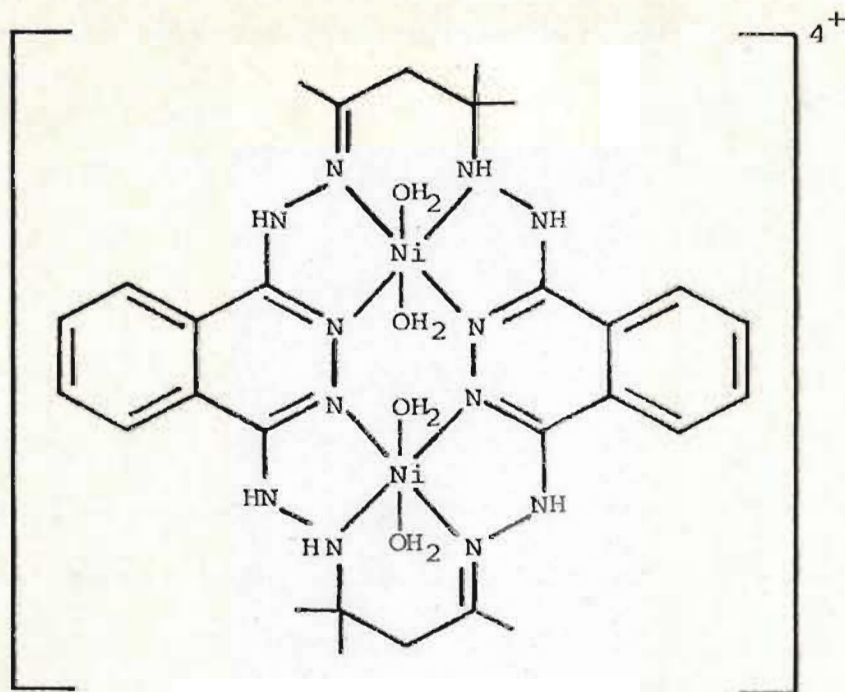


Fig. 8  
PROPOSED STRUCTURE FOR THE  
NICKEL(II) COMPLEX OF TAPH

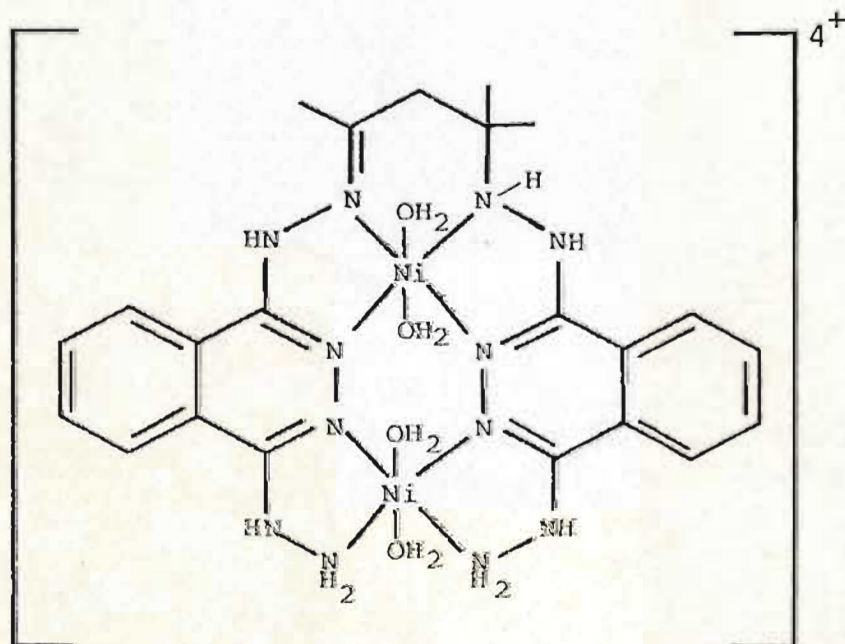


Fig. 9  
PROPOSED STRUCTURE FOR THE  
NICKEL(II) COMPLEX OF DAPH

The physical data for these systems indicate the nickel atoms are in octahedral or pseudo-octahedral fields. These paramagnetic complexes exhibit magnetic moments which lie below the accepted range for six-coordinate nickel(II).<sup>19</sup> As with the case of the nickel(II) complexes of DHPH<sup>15</sup>, it is assumed the lower magnetic moments are due to anti-ferromagnetic coupling through the ligand backbone.

Sullivan and Palenik<sup>20</sup> report a binuclear nickel(II) complex of the hexadentate ligand 1,4-dihydrazinophthalazine bis(2'-pyridine-carboxaldimine) (DHPHTH) (Fig. 10). The electronic spectroscopic properties of the complex are not discussed, but the magnetic moment of 2.74 B.M. is similar to those of the closely related DHPH systems. The low magnetic moment of the DHPHTH complex is not speculated upon, as temperature dependent magnetic susceptibility data were unavailable.

In the present study it was hoped to produce further examples of binuclear metal complexes in which the metal centres were close enough to exhibit antiferromagnetic exchange. Such systems are of potential importance in providing information relevant to studies of naturally occurring binuclear metalloprotein systems, e.g. hemo-cyanin and hemerythrin.

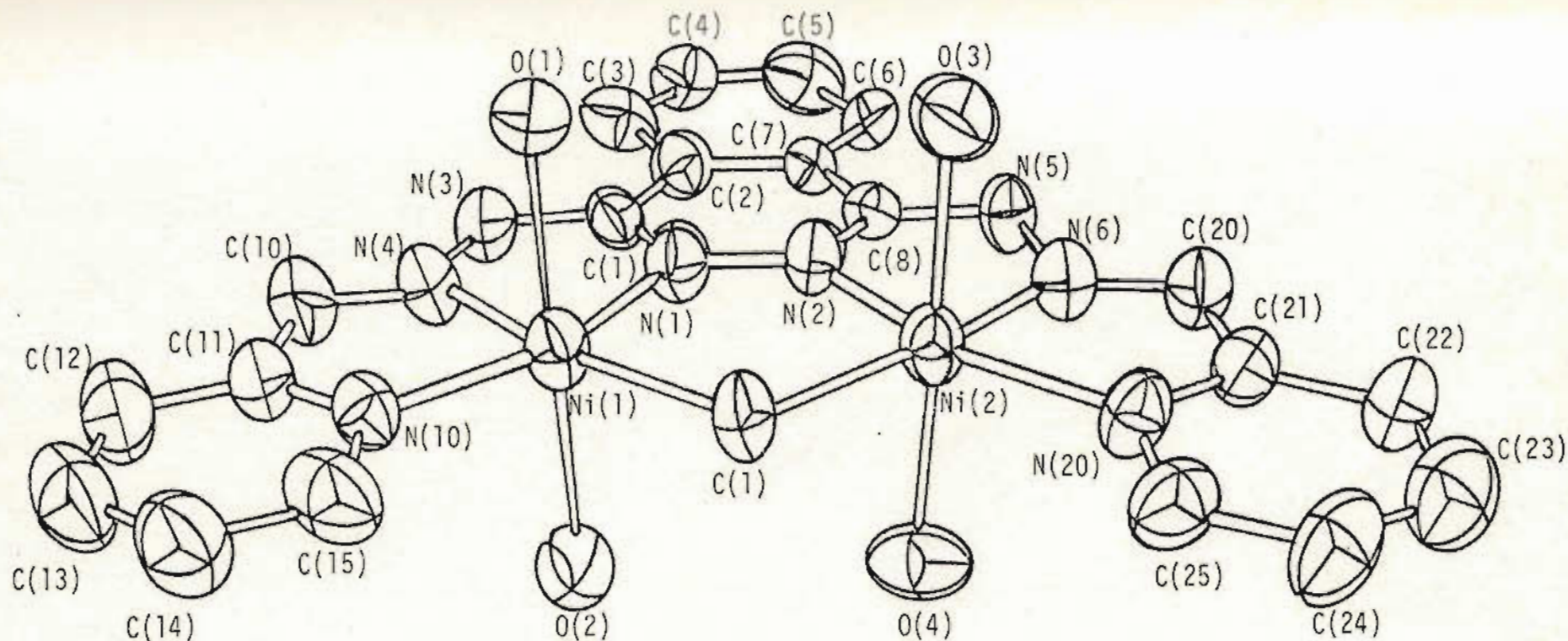


Fig. 10

ORTEP drawing of  $\mu$ -chloro-tetraaqua[1,4-dihydrazinophthalazine bis(2'-pyridinecarboxaldimine)]dinickel(II)cation. The chloride anions and the two water molecules have not been included for clarity.

TABLE 3

MAGNETIC PARAMETERS OF SOME NICKEL COMPLEXES WITH DPPN,  
Me<sub>2</sub>DPPN AND DHPH

COMPOUND <sup>a</sup>	$\mu_{\text{eff}}$ (300 K)	g	-J (cm <sup>-1</sup> )
Ni(DPPN)(NO <sub>3</sub> ) <sub>2</sub> ·H <sub>2</sub> O	2.91	2.21	23.5
Ni(DPPN)(ClO <sub>4</sub> ) <sub>2</sub> ·2H <sub>2</sub> O	2.91	2.15	14.7
Ni <sub>2</sub> (DPPN)(SO <sub>4</sub> ) <sub>2</sub> ·5H <sub>2</sub> O	2.87	2.18	12.3
Ni <sub>2</sub> (Me <sub>2</sub> DPPN)(NO <sub>3</sub> ) <sub>4</sub> ·2H <sub>2</sub> O	2.89	2.18	20.7
Ni <sub>2</sub> (Me <sub>2</sub> DPPN)(NO <sub>3</sub> ) <sub>4</sub> ·H <sub>2</sub> O·CH <sub>3</sub> OH	2.91	2.18	18.5
Ni(DHPH)Cl <sub>2</sub> ·3H <sub>2</sub> O	2.82	2.15	22.3
Ni(DHPH)Br <sub>2</sub> ·3H <sub>2</sub> O	2.79	2.16	23.8
Ni(DHPH)I <sub>2</sub> ·3H <sub>2</sub> O	2.81	2.14	21.3
Ni(DHPH)Cl <sub>2</sub> ·2H <sub>2</sub> O	2.80	2.14	23.5
Ni(DHPH)Br <sub>2</sub> ·2H <sub>2</sub> O	2.84	2.19	24.5
Ni(DHPH)Cl <sub>2</sub> ·0.5H <sub>2</sub> O	2.87	2.19	23.6
Ni(DHPH)Br <sub>2</sub> ·H <sub>2</sub> O	2.89	2.21	23.6
Ni(DHPH)I <sub>2</sub> ·H <sub>2</sub> O	2.84	2.18	24.0

SOURCE: Reference 15.

<sup>a</sup> All 1:1 (metal:ligand) complexes are binuclear.

ELECTRONIC AND MAGNETIC PROPERTIES OF NICKEL(II)

The outer shell configuration of nickel(II) is  $3d^8$ , which gives rise to the free ion spectroscopic states  $^3F$ ,  $^1D$ ,  $^3P$ ,  $^1G$ ,  $^1S$  (in order of increasing energy). The way in which these terms are split, and hence the spectral and magnetic properties of the complex depend on the stereochemistry of the nickel ion. (see Fig. 11)

Six-coordinate nickel(II) complexes are almost always high spin, and have regular or distorted octahedral symmetries. In an octahedral environment, the  $^3F$  term splits into three terms ( $^3T_{1g}$ ,  $^3T_{2g}$ ,  $^3A_{2g}$ ) (Fig. 12).<sup>21</sup> As may be seen from Fig. 12, there are three spin-allowed transitions expected from the  $^3A_{2g}$  ground state:

$$^3T_{2g} \leftarrow ^3A_{2g} \quad \nu_1 = 10 Dq$$

$$^3T_{1g}(F) \leftarrow ^3A_{2g} \quad \nu_2 = 15Dq + (15/2)B - (1/2) [(15B-6Dq)^2 + 64(Dq)^2]^{1/2}$$

$$^3T_{1g}(P) \leftarrow ^3A_{2g} \quad \nu_3 = 15Dq + (15/2)B + (1/2) [(15B-6Dq)^2 + 64(Dq)^2]^{1/2}$$

These transitions are usually observed in the regions 7,000 - 13,000  $\text{cm}^{-1}$  ( $\nu_1$ ), 11,000 - 20,000  $\text{cm}^{-1}$  ( $\nu_2$ ), and 20,000 - 28,000  $\text{cm}^{-1}$  ( $\nu_3$ ).

The term "B" in the equations for the transition energies is the Racah parameter, which arises from the difference in energy between free ion states of the same spin multiplicity. This difference in energy results from electron-electron repulsion, and the value of B for a complex (B') is always smaller than B for the free ion, due to delocalisation of metal electrons over molecular orbitals that encompass the entire molecule, including the ligand(s). The ratio of  $B'/B = \beta$  of

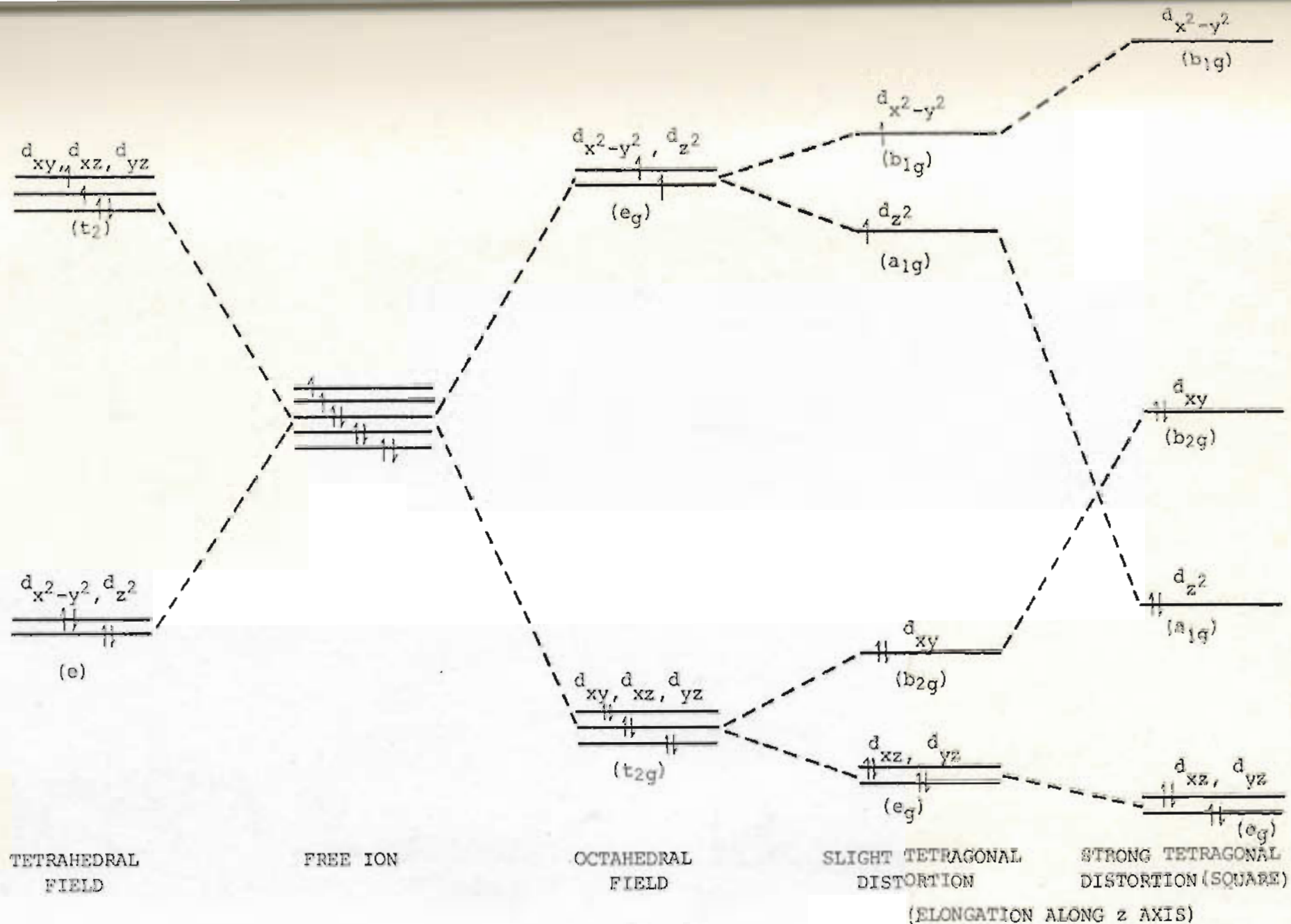


Fig. 11

CRYSTAL FIELD SPLITTING DIAGRAMS FOR NICKEL (II) IONS IN VARIOUS CRYSTAL FIELDS  
(NOT DRAWN TO SCALE)

a related series of complexes is a measure of the covalency of the metal-ligand bond, the smaller  $\beta$ , the more covalent the bond, and vice versa. The value of  $10Dq$  depends on the ligand(s) and can vary over a wide range e.g.  $10Dq$  for  $NiBr_2$  is  $6,800\text{ cm}^{-1}$ ,<sup>22</sup> while that for  $[Ni(\text{phen})_3]^{2+}$  is  $12,700\text{ cm}^{-1}$ .<sup>23</sup>

Spin forbidden transitions are sometimes observed in the electronic spectra of octahedral nickel(II) complexes. The  $^1E_g \leftarrow ^3A_{2g}$  absorption appears in the  $11,000 - 15,000\text{ cm}^{-1}$  region, and that of  $^1T_{2g} \leftarrow ^3A_{2g}$  in the  $17,000 - 22,000\text{ cm}^{-1}$  region. The absorptions corresponding to the transitions  $^3T_{2g} \leftarrow ^3A_{2g}$  and  $^3T_{1g}(P) \leftarrow ^3A_{2g}$  are usually symmetric, but the  $^3T_{1g}(F) \leftarrow ^3A_{2g}$  band often has a shoulder, or even appears as a doublet, especially when  $Dq/B$  approaches unity. It has been suggested that the doublet structure is due to a gain in the intensity of the transition  $^1E_g \leftarrow ^3A_{2g}$  through configurational interaction with the  $^3T_{1g}(F)$  level<sup>23,24</sup>, or possibly through spin-orbit coupling.<sup>25</sup>

Pseudo-octahedral six-coordinate complexes of the type  $NiL_4X_2$  have spectra characteristic of octahedral nickel(II). The  $\nu_2$  and  $\nu_3$  bands are not usually affected by the lower symmetry, but a splitting of  $2,000 - 2,500\text{ cm}^{-1}$  is often observed in the  $\nu_1$  band of *trans*  $NiL_4X_2$  complexes with  $D_{4h}$  symmetry, assigned to the transitions  $^3B_{2g} \leftarrow ^3B_{1g}$  and  $^3E_g \leftarrow ^3B_{1g}$  (tetragonal components of the octahedral  $^3T_{2g}$  level). A smaller splitting is observed for "cis-octahedral" complexes. The effects of these distortions from octahedral symmetry on the energy levels of the nickel(II) ion have been illustrated by Furlani<sup>26</sup>.

Octahedral complexes of nickel(II) have a triplet ground state  $^3A_{2g}$  and are usually paramagnetic. Although in theory there



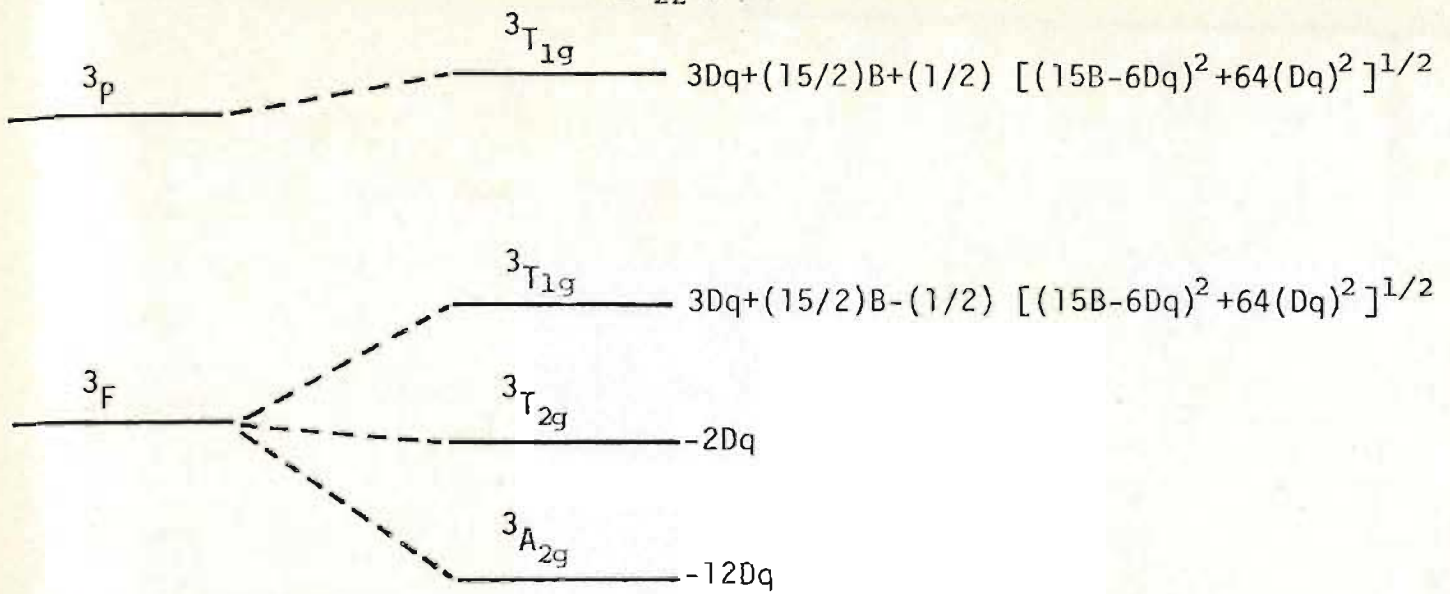


Fig. 12

TRIPLET TERMS ARISING FROM NICKEL (II) IONS IN OCTAHEDRAL FIELDS

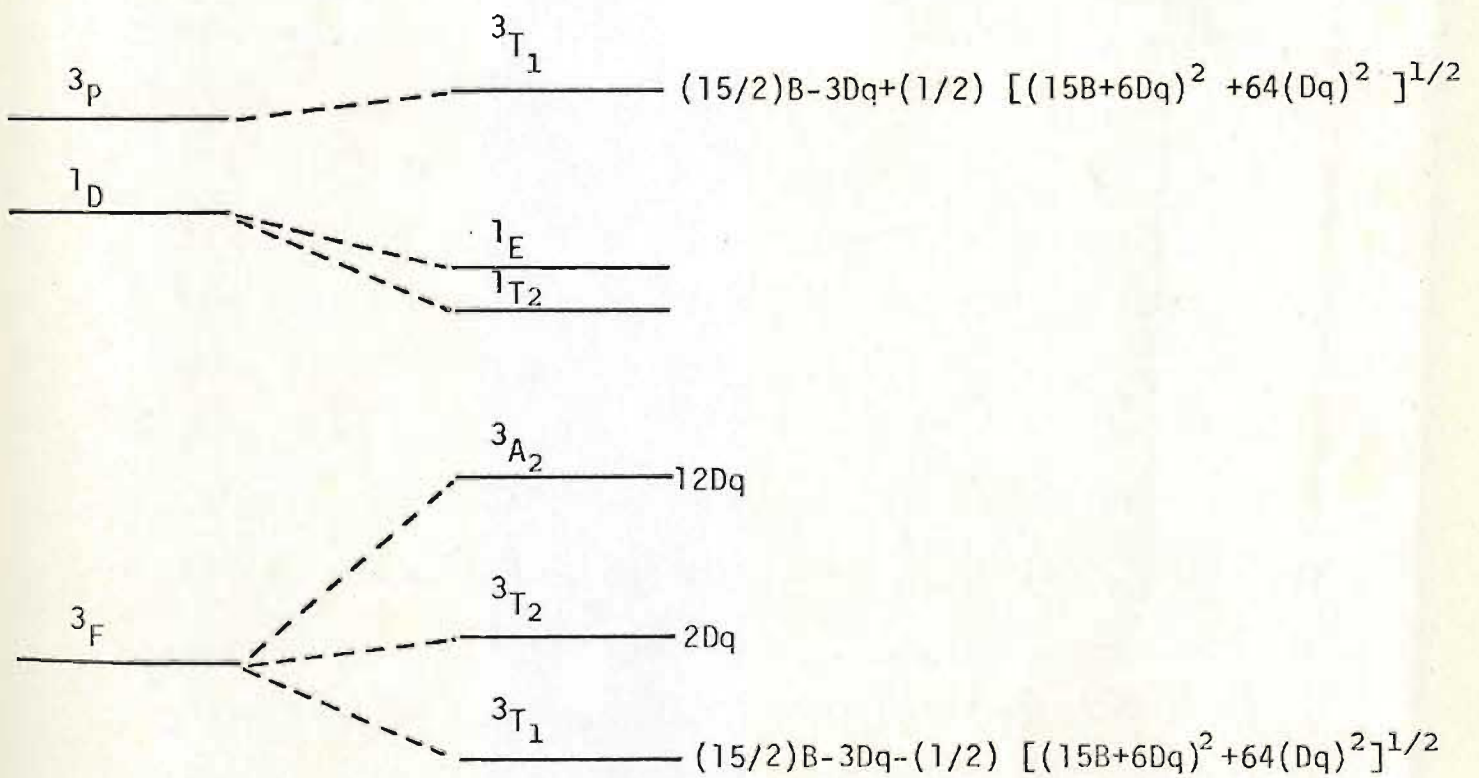


Fig 13

TRIPLET TERMS ARISING FROM NICKEL (II) IONS IN TETRAHEDRAL FIELDS

should be no orbital contribution to the magnetic moment, in actual fact there is because of spin-orbit coupling. Because of this orbital contribution, the magnetic moment is always greater than the spin-only value of 2.83 B.M., usually ranging from 2.9 to 3.3 B.M. The magnetic moment does not vary appreciably with temperature change or minor distortions from octahedral symmetry. There are some six-coordinate complexes of nickel(II) that are diamagnetic, perhaps the most studied being bis(o-phenylenebisdimethylarsine)nickel(II) iodide. In this complex the iodine atoms are trans to each other, and the nickel iodine distance is greater than the sum of the atomic radii<sup>27</sup>, also, iodine and the arsine are far from each other in the spectrochemical series. These two effects combine to cause a strong tetragonal distortion, the net result being that the complex is essentially square-planar.

The outer shell electronic configuration of tetrahedral nickel(II) is  $e^4 t_2^4$ , and has a free ion splitting as shown in Fig. 13. As with octahedral complexes, there are three spin-allowed transitions expected in the electronic spectra of tetrahedral nickel(II) complexes, except in this case they arise from a  $^3T_1$  ground state. Since the crystal field splitting is only 4/9 that of an octahedral field, the electronic transitions shift toward the infrared when compared with those of an octahedral complex. The absence of a centre of symmetry in the tetrahedral field causes the absorptions to be more intense than those of an octahedral field. The highest energy transition,  $^3T_1(P) \leftarrow ^3T_1$ , is usually observed as a very broad envelope near  $15,000 \text{ cm}^{-1}$ , with shoulders due to spin-forbidden bands.<sup>28</sup> The  $^3A_2 \leftarrow ^3T_1$  absorption

appears around  $7,000 \text{ cm}^{-1}$ . The low energy  ${}^3T_2 \leftarrow {}^3T_1$  transition is frequently not observed, as it lies in the range of conventional infrared, and can be masked by vibrational transitions. The orbital degeneracy of the  ${}^3T_1$  ground state of the tetrahedral complexes causes the magnetic moment to be higher than the spin-only value through orbital contribution; experimental values range from 3.2 to 4.1 B.M. and are temperature dependent.

The square-planar configuration for nickel(II) complexes is energetically less favourable than the tetrahedral in terms of spin-pairing energy and minimisation of electrostatic repulsion. The major stabilisation factor for such complexes is strong nickel-ligand covalent bonding (both  $\sigma$  and  $\pi$ ). Square planar complexes of nickel(II) may have either of two ground states:  $e_g^4 a_{1g}^2 b_{2g}^2$  (spin singlet state  ${}^1A_{2g}$ ) or  $e_g^4 a_{1g}^2 b_{2g}^1 b_{1g}^1$  (spin triplet state  ${}^3A_{2g}$  and an excited state  ${}^1A_{2g}$ ).<sup>28</sup> The low spin state is favoured if the separation between the  $d_{x^2-y^2}$  and  $d_{xy}$  orbitals is greater than  $10,000 \text{ cm}^{-1}$ .

The spectra of square planar complexes of nickel(II) usually have a strong band ( $\epsilon = 50 - 500 \text{ l cm}^{-1} \text{ mole}^{-1}$ ) in the region  $15,000$  to  $23,000 \text{ cm}^{-1}$  ( ${}^1A_{2g} \leftarrow {}^1A_{1g}$ ) and a second absorption between  $23,000$  and  $27,000 \text{ cm}^{-1}$  ( ${}^1B_{1g} \leftarrow {}^1A_{1g}$ ). A weaker band, believed to be due to a spin-forbidden transition is sometimes found in the area  $11,000 - 13,000 \text{ cm}^{-1}$ . The most notable difference between the spectrum of a square planar complex and that of an octahedral one is the absence of any absorption below  $10,000 \text{ cm}^{-1}$  in the case of the former. The lack of such a band indicates the energy separation between the  $d_{x^2-y^2}$

and  $d_{xy}$  orbitals is greater than  $10,000 \text{ cm}^{-1}$ , and the complex will be in a low spin state, and hence diamagnetic.

#### NICKEL(II) COMPLEXES OF PAP

Aqueous solutions of nickel(II) salts react readily with PAP to form a series of complexes of general formulae  $\text{PAP}_2\text{Ni}_2\text{X}_4 \cdot n\text{H}_2\text{O}$  ( $\text{X} = \text{Cl}, \text{Br}, \text{I}, \text{NO}_3$ ;  $n = 0-7$ ), or  $\text{PAP}_2\text{Ni}_2(\text{OH})\text{Y}_3 \cdot n\text{H}_2\text{O}$  ( $\text{Y} = \text{NO}_3, \text{ClO}_4, \text{BF}_4$ ;  $n = 0-2$ ). The solubilities of these complexes in water are quite variable, the chloride complex being the most soluble and the perchlorate the least. The complexes are also soluble in methanol and ethanol to varying degrees, but are insoluble in other common organic solvents, except pyridine. A sample of the bromide complex "recrystallised" from pyridine formed a pale blue powder. The infrared spectrum of this compound indicates it is a pyridine complex, presumably the blue complex,  $\text{Ni}(\text{pyridine})_4\text{Br}_2$ . The infrared absorptions associated with the ligand in these nickel complexes are similar to those of  $\text{PAPCu}_2\text{Cl}_3(\text{OH}) \cdot \text{H}_2\text{O}$ , indicating structural similarity of the ligand environments between the nickel complexes and that of the copper chloride complex. (see Fig. 3) The infrared spectra of all the nickel PAP complexes show shifts of  $20-30 \text{ cm}^{-1}$  to higher energy in the pyridine ring breathing mode absorption (Table 4); by analogy with the copper hydroxy chloride complex it is assumed the ligand in these complexes is also tetradentate, coordinating via the phthalazine and pyridine nitrogens. Electronic spectra indicate the ligand moieties of all the nickel complexes to be neutral. (see section on Electronic Spectra).

## INFRARED SPECTRAL DATA

### NICKEL HALIDE COMPLEXES

The infrared spectra of the PAP-nickel chloride and bromide complexes are almost superimposable, while that of the iodide is very similar. As the metal:ligand ratio is 1:1 (see experimental section), the presence of tetradentate PAP in the nickel complexes indicates that the molecular formula is twice the empirical formula suggested by elemental analyses, and should be written  $\text{PAP}_2\text{Ni}_2\text{X}_4 \cdot n\text{H}_2\text{O}$ .

The high energy portions of the infrared spectra of the chloride and bromide complexes show a broad absorption in the range 3600-3100  $\text{cm}^{-1}$ . Although it is difficult to make specific assignments in this area a shoulder around 3500  $\text{cm}^{-1}$  is associated with water, while absorptions in the range 3260-3430  $\text{cm}^{-1}$  are assigned to N-H stretch, and an absorption between 3160 and 3180  $\text{cm}^{-1}$  is assigned to aromatic C-H stretch (Table 4). The nickel iodide complex shows no absorptions due to water, and elemental analyses are consistent with an anhydrous complex (see section on experimental procedure). The spectrum of the iodide complex shows "shoulder" absorptions similar to those of the chloride and bromide complexes, which may be assigned to N-H and C-H stretching vibrations.

The low energy regions of the infrared spectra of the halide complexes prepared do not contain evidence of nickel-halogen vibrations. The iodide complex did not show Ni-I stretching absorptions above 200  $\text{cm}^{-1}$ .

### NICKEL NITRATE COMPLEXES

Two complexes were isolated from the PAP-nickel nitrate reaction solution: purple needle-like crystals and green rhombic crystals.

The electronic and infrared spectra confirm that these are distinct complexes and not just different hydrated forms. Elemental analyses indicate the formulae to be  $\text{PAP}_2\text{Ni}_2(\text{OH})(\text{NO}_3)_3$  and  $\text{PAP}_2\text{Ni}_2(\text{NO}_3)_4$  respectively.

The high energy regions of the infrared spectra of both nitrate complexes show various N-H and C-H "shoulder absorptions" between 3300 and  $3000\text{ cm}^{-1}$ . Again, it is difficult to make specific assignments, but by comparison with the spectrum of the ligand, some tentative assignments were made (Table 4). No absorptions were observed around  $3500\text{ cm}^{-1}$  in the spectra of the vacuum dried complexes, indicating the absence of coordinated water or water of crystallization.

The infrared spectra of compounds with ionic nitrate groups have three bands:  $\nu_2$  ( $A_2'', D_{3h}$ ),  $\nu_3$  ( $E', D_{3h}$ ) and  $\nu_4$  ( $E', D_{3h}$ ). The  $\nu_1$  ( $A_1', D_{3h}$ ) band is usually inactive in the infrared, but it is sometimes allowed because of crystal interactions.<sup>29</sup> For mono- and bidentate nitrate groups (i.e. "nitrato" groups) the symmetry is reduced to  $C_{2v}$  and all bands become infrared active. The reduction in symmetry causes shifts in band positions and lifts the degeneracy of the  $\nu_3$  and  $\nu_4$  bands. The two non-degenerate bands arising from each of the  $\nu_3$  and  $\nu_4$  ( $D_{3h}$ ) absorptions show greater separation for bidentate than monodentate nitrate. The  $\nu_1 + \nu_4$  ( $D_{3h}$ ) combination band, occurring in the  $1700\text{-}1800\text{ cm}^{-1}$  region, is frequently of use in providing structural information. A sharp band arises from ionic nitrate but splitting is observed for coordinated nitrate. The separation of these two frequencies depends on the strength of the interaction

between the metal and the nitrate group, bidentate giving a wider separation ( $20-56 \text{ cm}^{-1}$ ) than unidentate nitrate ( $5-26 \text{ cm}^{-1}$ ).<sup>30,31</sup>

Identification of the nitrate absorptions in the PAP-nickel complexes was made by comparing the spectra of the nitrate complexes with those of the other PAP-nickel complexes. However, the complexity of the infrared spectrum of PAP itself makes identification of all nitrate bands difficult and it is possible that some nitrate absorptions are masked by ligand (PAP) absorptions.

Some fundamental nitrate bands for the two complexes are observed (Table 5) and indicate the presence of ionic and unidentate nitrate groups in the case of the trinitrate, and ionic, unidentate and bidentate groups for the tetranitrate. Other fundamental absorptions are probably masked by ligand vibrations. Only a weak single combination band at  $1760 \text{ cm}^{-1}$  was observed for the tetranitrate complex, confirming ionic nitrate. In the case of the trinitrate complex combination bands associated with both ionic and monodentate nitrate were observed.

A weak absorption occurring at  $3450 \text{ cm}^{-1}$  in the trinitrate complex is assigned to O-H stretch of bridging hydroxide. A band occurring between  $3300$  and  $3400 \text{ cm}^{-1}$  in the spectrum of  $\text{K}_4[(\text{ox})_2\text{Co}(\text{OH})_2\text{Co}(\text{ox})_2]$  has been assigned by Nakamoto to a stretching vibration of bridging hydroxide<sup>32</sup>, whereas Scargill reports this band to occur between  $3200$  and  $3500 \text{ cm}^{-1}$  in various hydroxy complexes of ruthenium.<sup>33</sup>

Assuming that each nickel ion is six-coordinate in these systems (see section on electronic spectra) and that PAP is acting in a tetradentate manner, the role of the nitrate groups can be proposed. As

the trinitrate seems to have a bridging hydroxide, the one remaining coordination site on each nickel atom could be occupied by monodentate nitrate groups. The tetranitrate appears to be more complex in that it appears to have ionic, unidentate and bidentate nitrate groups. Molecular models indicate that the nickel atoms in these compounds may be bridged by either hydroxy or bidentate nitrate groups to form a "cis-" or "trans-" dimeric binuclear structure.

#### NICKEL PERCHLORATE COMPLEX

The spectrum of the PAP-nickel perchlorate complex is blank between 970 and 1000  $\text{cm}^{-1}$ , but has a band at 1015  $\text{cm}^{-1}$  which has been assigned to a shifted pyridine ring breathing mode absorption. The high energy region of the spectrum shows a broad absorption between 3700 and 3400  $\text{cm}^{-1}$ , and peaks at 3360 and 3100  $\text{cm}^{-1}$ . The broad, high energy absorption suggests the presence of water, and elemental analyses are consistent with three water molecules per molecule of complex, or alternatively two water molecules and a hydroxide group. The band at 3360  $\text{cm}^{-1}$  has been assigned to N-H stretch.

Tetrahedral (ionic) perchlorate has two infrared active modes:  $\nu_3$  ( $T_2, T_d$ ), a strong absorption around 1100  $\text{cm}^{-1}$  (occasionally split)<sup>34</sup>, and  $\nu_4$  ( $T_2, T_d$ ), a sharp absorption around 630  $\text{cm}^{-1}$ <sup>35</sup>. The  $\nu_1$  ( $A_1, T_d$ ) band is theoretically only Raman active, but usually shows up as a weak absorption at 930  $\text{cm}^{-1}$ <sup>35</sup>; this band becomes weakly allowed if the symmetry of the crystal field about the ion is lower than that of the ion itself. For monodentate perchlorate, the symmetry of the ion is reduced to  $C_{3v}$ . The triply degenerate



$\nu_3$  ( $T_2, T_d$ ) splits into  $\nu_1$  ( $A_1, C_{3V}$ ) and  $\nu_4$  ( $E, C_{3V}$ ); so two strong absorptions between 1000 and 1200  $\text{cm}^{-1}$  are expected, as well as a moderately strong band between 940 and 890  $\text{cm}^{-1}$ , the "forbidden"  $\nu_1$  ( $A_1, T_d$ ) now becoming allowed as  $\nu_2$  ( $A_1, C_{3V}$ )<sup>35</sup>. Bidentate perchlorate has a symmetry of  $C_{2V}$ , causing further splitting and producing three intense absorptions between 1000 and 1200  $\text{cm}^{-1}$ :  $\nu_1$  ( $A_1, C_{2V}$ ),  $\nu_6$  ( $B_1, C_{2V}$ ),  $\nu_8$  ( $B_2, C_{2V}$ ). The relationships between these bands in the various symmetries are shown in Table 6.

The anion absorptions of the perchlorate complex were assigned by comparing the spectra of the perchlorate, tetrafluoroborate and nitrate complexes. The absorptions assigned to the perchlorate group (Table 5) indicate ionic perchlorate. The electronic spectrum of the complex indicates the nickel atoms are in a distorted octahedral environment. Since the perchlorate groups are ionic (uncoordinated) the two remaining coordination sites of each nickel atom must be occupied by a hydroxide bridge and a water molecule.

#### NICKEL TETRAFLUOROBORATE COMPLEX

The infrared and electronic spectra of the tetrafluoroborate complex are very similar to those of the perchlorate complex, and it is assumed that these complexes are isostructural.

It is impossible to determine the position of the pyridine ring breathing mode in this complex, as it is masked by a broad intense absorption of the tetrafluoroborate ion. However, as with the other complexes discussed, the ligand is assumed to function in a tetradentate manner, coordinating to the two nickel atoms via both

phthalazine and pyridine nitrogen atoms. The high energy portion of the spectrum shows an absorption around  $3100\text{ cm}^{-1}$ , which is assigned to aromatic C-H stretch. The spectrum also shows an intense, sharp absorption at  $3370\text{ cm}^{-1}$ , which shifts to  $2490\text{ cm}^{-1}$  when the complex is prepared in  $\text{D}_2\text{O}$ . This absorption has been assigned to exocyclic N-H stretch. An intense doublet with peaks at  $3460\text{ cm}^{-1}$  and  $3505\text{ cm}^{-1}$  may be assigned to  $\nu_1$  (symm. str.) and  $\nu_2$  (assym. str.) of coordinated water, or alternatively, one of the bands may be due to bridging hydroxide and the other to water.

The tetrafluoroborate ion, belonging to the same point group as the perchlorate ion, has the same fundamental vibrations in terms of symmetry species. However, as naturally occurring boron consists of  $\text{B}^{10}$  and  $\text{B}^{11}$  in a ratio of 1:4, the spectrum of the tetrafluoroborate ion is further complicated by isotopic splitting of the  $\nu_3$  ( $\text{T}_2, \text{T}_d$ ) and  $\nu_4$  ( $\text{T}_2, \text{T}_d$ ) absorption modes.<sup>36</sup>

The only positive spectral evidence of the tetrafluoroborate ion in the PAP complex is a broad, intense absorption between  $1150\text{ cm}^{-1}$  and  $900\text{ cm}^{-1}$ , with shoulders at  $1095\text{ cm}^{-1}$ ,  $1060\text{ cm}^{-1}$  and  $1000\text{ cm}^{-1}$  (see Table 5). This band is assigned to  $\nu_3$  ( $\text{T}_2, \text{T}_d$ ) of ionic tetrafluoroborate, split by symmetry and isotope effects.

The far IR regions of the infrared spectra of the PAP-nickel complexes reveal no definite structural information.

TABLE 4

## LIGAND AND WATER VIBRATIONS OF THE PAP-NICKEL COMPLEXES

COMPOUND	$\nu_{\text{H}_2\text{O}}$ ( $\text{cm}^{-1}$ )	$\nu_{\text{N-H}}$ ( $\text{cm}^{-1}$ )	$\nu_{\text{C-H}}$ ( $\text{cm}^{-1}$ )	PYRIDINE RING ( $\text{cm}^{-1}$ ) BREATHING MODE
$[\text{PAP}_2\text{Ni}_2(\text{H}_2\text{O})_4]\text{Cl}_4 \cdot 3\text{H}_2\text{O}$	3500 (m.st., v.br.)	3380 (m.st., br.) 3280 (m.st., br.)	3160 (wk, br.) 3060 (wk, br.)	1018
$[\text{PAP}_2\text{Ni}_2(\text{H}_2\text{O})_4]\text{Br}_4$	3500 (m.st., v.br.)	3400 (m.st., v.br.) 3280 (m.st., v.br.)	3180 (m.st., v.br.) 3060 (m.st., v.br.)	1012
$[\text{PAP}_2\text{Ni}_2\text{I}_4]$		3400 (m.st., v.br.) 3270 (m.st., v.br.)	3180 (m.st., v.br.) 3070 (m.st., v.br.)	1010
$[\text{PAP}_2\text{Ni}_2(\text{OH})(\text{NO}_3)_3]$	3450 (wk, $\nu_{\text{O-H}}$ )	3300 (m.st.) 3200 (wk.)	3170 (wk.) 3140 (wk.) 3080 (wk., br.)	1008
$[\text{PAP}_2\text{Ni}_2(\text{NO}_3)_4]$		3270 (m.st., br.) 3200 (m.st., br.)	3140 (m.st., br.) 3070 (m.st., br.)	1012
$[\text{PAP}_2\text{Ni}_2(\text{OH})(\text{H}_2\text{O})_2](\text{ClO}_4)_3$	3700-3400 (st.)	3360 (st. br.)	3100 (m.st., br.)	1015
$[\text{PAP}_2\text{Ni}_2(\text{OH})(\text{H}_2\text{O})_2](\text{BF}_4)_3$	3505, 3460 (dbl., st., br.)	3370 (st., sh.)	3100 (m.st., br.)	1015
$\text{PAPCu}_2(\text{OH})\text{Cl}_3 \cdot \text{H}_2\text{O}$	3600 (m.st., sh) 3560, 3580 (dbl., m.st.)	3300 (st., sh.)	3200 (wk., sh.) 3060, 3100 (wk., br.)	1020

br., broad; dbl., doublet; m.st., medium strong; st., strong; sh., sharp; wk., weak; v.br., very broad

TABLE 5

## ANION ABSORPTIONS OF PAP-NICKEL COMPLEXES

COMPOUND	NITRATE			$\nu_1 + \nu_4^*$ ( $\text{cm}^{-1}$ )
	IONIC ( $\text{cm}^{-1}$ )	UNIDENTATE ( $\text{cm}^{-1}$ )	BIDENTATE ( $\text{cm}^{-1}$ )	
$[\text{PAP}_2\text{Ni}_2(\text{OH})(\text{NO}_3)_3]$	827	1315, 900		1750(i), 1755(u), 1738(u)
$[\text{PAP}_2\text{Ni}_2(\text{NO}_3)_4]$	828	1315, 1000	1530	1760(i)

## PERCHLORATE AND TETRAFLUOROBORATE

COMPOUND	$\nu_1(A_1, T_d)$ ( $\text{cm}^{-1}$ )	$\nu_3(T_2, T_d)$ ( $\text{cm}^{-1}$ )	$\nu_4(T_2, T_d)$ ( $\text{cm}^{-1}$ )
$[\text{PAP}_2\text{Ni}_2(\text{OH})(\text{H}_2\text{O})_2](\text{ClO}_4)_3$	930	1025 - 1150	620
$[\text{PAP}_2\text{Ni}_2(\text{OH})(\text{H}_2\text{O})_2](\text{BF}_4)_3$		900 - 1150	

\* i. characteristic of ionic nitrate

u. characteristic of unidentate nitrate

TABLE 6<sup>1</sup>VIBRATIONS OF THE (ClO<sub>4</sub>) GROUP IN DIFFERENT SYMMETRY ENVIRONMENTS<sup>†</sup>

SYMMETRY	$\nu_2$	$\nu_6$	$\nu_1$	$\nu_4$	$\nu_3$	$\nu_5$
-O*-ClO <sub>3</sub> C <sub>3v</sub>	A <sub>1</sub> (I.,R.)	E(I.,R.)	A <sub>1</sub> (I.,R.)	E(I.,R.)	A <sub>1</sub> (I.,R.)	E(I.,R.)
	ClO Str.	Rocking	ClO <sub>2</sub> Sym. Str.	*OCl Asym. Bend.	ClO <sub>3</sub> Sym. Bend.	ClO <sub>2</sub> Asym. Bend.

ClO <sub>4</sub> <sup>-</sup>	Td	$\nu_1$ A <sub>1</sub> (R) Sym. Str.	$\nu_2$ E(R) Sym. Bend.	$\nu_3$ T <sub>2</sub> (I.,R.) Asym. Str.	$\nu_4$ T <sub>2</sub> (I.,R.) Asym. Bend.		
		932	460	1110	626		
-O* ClO <sub>2</sub> -O*	C <sub>2v</sub>	$\nu_2$ A <sub>1</sub> (I.,R.) Cl O* O* Sym. Str.	$\nu_4$ A <sub>1</sub> (I.,R.) Cl O* O* Sym. Bend.	$\nu_1$ A <sub>1</sub> (I.,R.) ClO <sub>2</sub> Sym. Str.	$\nu_6$ B <sub>1</sub> (I.,R.) ClO <sub>2</sub> Asym. Str.	$\nu_8$ B <sub>2</sub> (I.,R.) Cl O* O* Asym. Str.	
				$\nu_5$ A <sub>2</sub> (R) Torsion	$\nu_3$ A <sub>1</sub> (I.,R.) ClO <sub>2</sub> Sym. Bend.	$\nu_7$ B <sub>1</sub> (I.,R.) Rocking	$\nu_9$ B <sub>2</sub> (I.,R.) Rocking

<sup>1</sup>From B.J. Hathaway A.E. Underhill; J. Chem. Soc., 3091 (1961).<sup>†</sup>I, infrared active. R, Raman active. O\* refers to coordinated oxygen atoms.

## ELECTRONIC SPECTRA

The solid state electronic spectra of the PAP-nickel complexes are all very similar, there being a broad absorption in the range 11,400 - 12,000  $\text{cm}^{-1}$ , and a sharper absorption between 17,500 and 18,500  $\text{cm}^{-1}$ . These two bands are assigned respectively to the  $\nu_1$  and  $\nu_2$  transitions of nickel(II) in an octahedral environment. The expected  $\nu_3$  absorption is masked by intense charge transfer bands of the ligand, which occur above 20,000  $\text{cm}^{-1}$ . In some cases the  $\nu_2$  absorption shows a weak shoulder band around 15,000  $\text{cm}^{-1}$ , which is assigned to the spin forbidden  ${}^1E_g \leftarrow {}^3A_{2g}$  transition. The assignments of the electronic transitions are shown in Table 7, along with the values of Dq and the Racah parameter, B.

At room temperature the solid state electronic spectrum of the chloride complex shows no obvious splitting of  $\nu_1$  although a shoulder does appear at low temperature. The solid state and aqueous solution spectra are identical and also conductivity data (Table 10) indicate the presence of ionic halide. These data indicate coordinated water in the solid state. For the nickel atoms in this binuclear, dimeric complex to be octahedral, the coordination environment around the metal must be  $\text{NiN}_4\text{O}_2$ , where O represents a coordinated water molecule. In the absence of any apparent splitting of  $\nu_1$ , the ligand molecules must be in a "cis" octahedral arrangement around the nickel atoms (see Introduction). In this respect the PAP-nickel chloride complex is similar to the binuclear monomeric complexes  $\text{Ni}_2(\text{DPPN})(\text{SO}_4)_2$  and  $\text{Ni}_2(\text{Me}_2\text{DPPN})(\text{NO}_3)_3 \cdot 2\text{H}_2\text{O}$  (see Introduction), which also show little splitting of  $\nu_1$ , and have been assigned a cis  $\text{Ni-N}_2\text{O}_4$  type structure.

The solid state electronic spectra of the rest of the PAP-nickel complexes are all similar to that of the chloride, indicating the coordination environment of the nickel atoms to be similar in all cases. For all of the complexes, except perhaps the iodide, four of the coordination sites around the nickel atom are occupied by ligand nitrogen atoms, while the remaining two are occupied by oxygen, either in the form of coordinated water, a hydroxy bridge, or coordinated nitrate groups. The differences in the groups occupying the fifth and sixth coordination sites apparently does not have a great influence on the electronic transitions of the nickel atom. The case of the iodide complex is anomalous, since a lower value of  $Dq$  would be expected, compared to the other complexes, if the iodine atoms were coordinated to the metal. That the value of  $Dq$  for the iodide complex is much the same as those of the other complexes may indicate the presence of coordinated water, although this is not confirmed by elemental analyses or infrared spectroscopy.

Some preparations of the nickel chloride and bromide complexes yielded products which, when dried, had an empirical formula  $PAPNiX_2 \cdot 1.5H_2O$ . The solid state electronic spectra of these complexes are similar to those of the corresponding tetraaquo species, and show the same solution spectra. Presumably these compounds contain a coordinated halide in the solid state, but this has little effect on the electronic environment of the nickel atom. In solution the coordinated halide becomes labile, and is replaced by a water molecule.

The solution spectra of the chloride (see Fig. 14), perchlorate and tetrafluoroborate complexes are essentially the same as their solid state analogues indicating the presence of the same species in both states. Conductance data indicate the coordinated anions in the nitrate complexes to be labile (see section on Conductance Studies), so in solution the nickel atoms are coordinated to water molecules instead of nitrate groups. The similarity of the electronic spectra of the nitrate complexes in solution to those of the solid state is not surprising, as the solid state spectra of the nitrate complexes are similar to that of the chloride, in which the nickel atoms are coordinated to water molecules. In the solution spectra of the bromide and iodide complexes, the  $\nu_2$  band remains unchanged from the solid state spectrum, but  $\nu_1$  appears as a broad absorption with two components around  $10,300\text{ cm}^{-1}$  and  $11,500\text{ cm}^{-1}$ . The  $\nu_1$  absorption is changed by the addition of concentrated HCl (see Fig. 15). As the acid is slowly added, the shoulder at  $10,300\text{ cm}^{-1}$  decreases in relative intensity, while that at  $11,500\text{ cm}^{-1}$  increases; an isosbestic point at  $10,500\text{ cm}^{-1}$  indicates an equilibrium exists in solution between the two species represented by the two components of  $\nu_1$ . The absorption at  $11,500\text{ cm}^{-1}$  indicates the presence of a tetraaquo PAP-nickel species in solution, as this is also the position of  $\nu_1$  of the chloride complex. The absorption at  $10,300\text{ cm}^{-1}$  does not represent  $\nu_1$  of a known nickel complex of PAP. During the preparation of the bromide complex, some PAP-hydrobromide was obtained (see Experimental section), indicating that the complex is capable of reacting with water to produce HBr. An



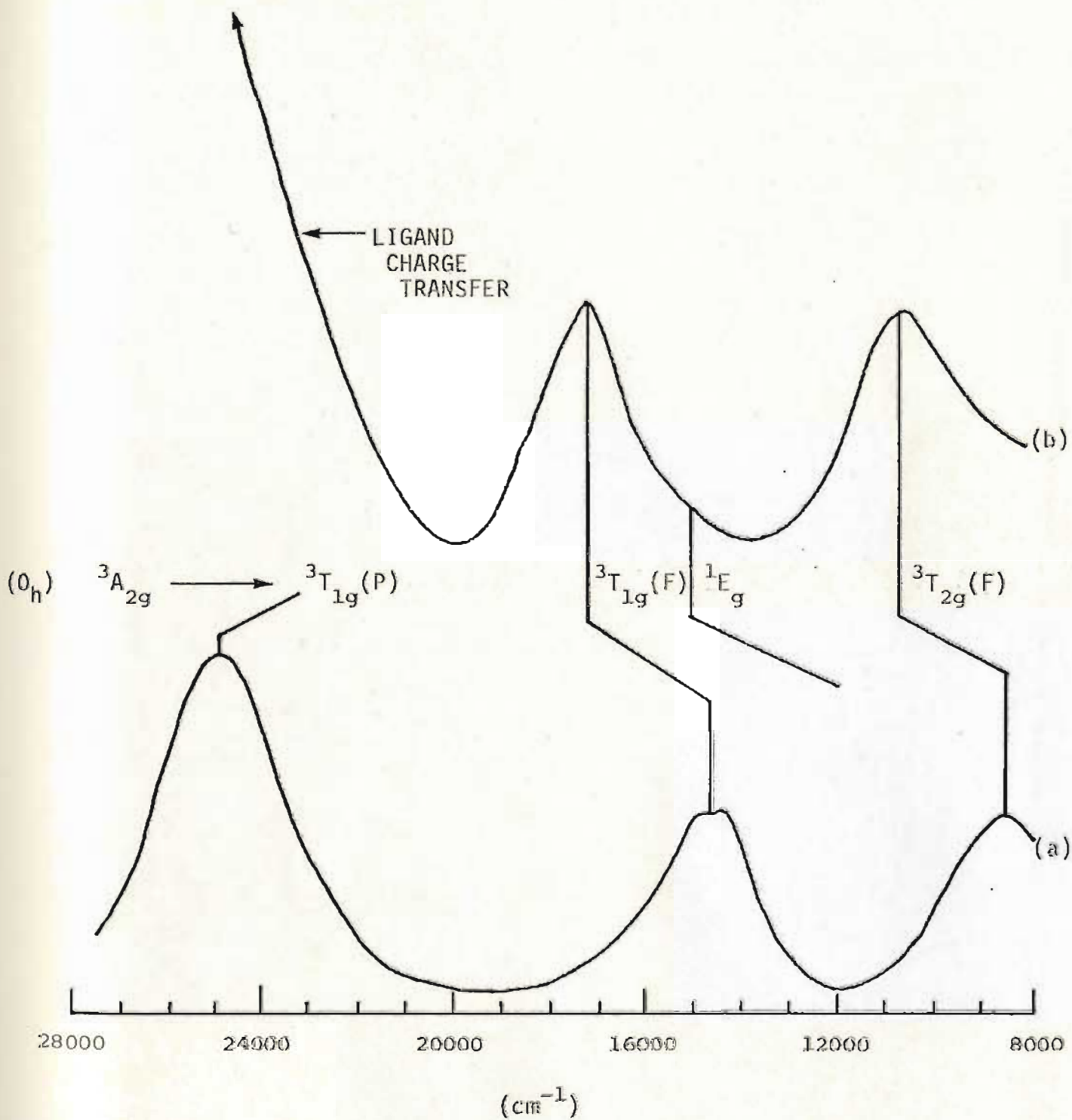


Fig. 14

A COMPARISON OF THE ELECTRONIC SPECTRUM OF  $[\text{Ni}(\text{H}_2\text{O})_6]^{2+}(\text{aq})$  (a), WITH THAT OF  $[\text{PAP}_2\text{Ni}_2(\text{H}_2\text{O})_4]\text{Cl}_4(\text{aq})$  (b) (ARBITRARY ABSORBANCE UNITS).

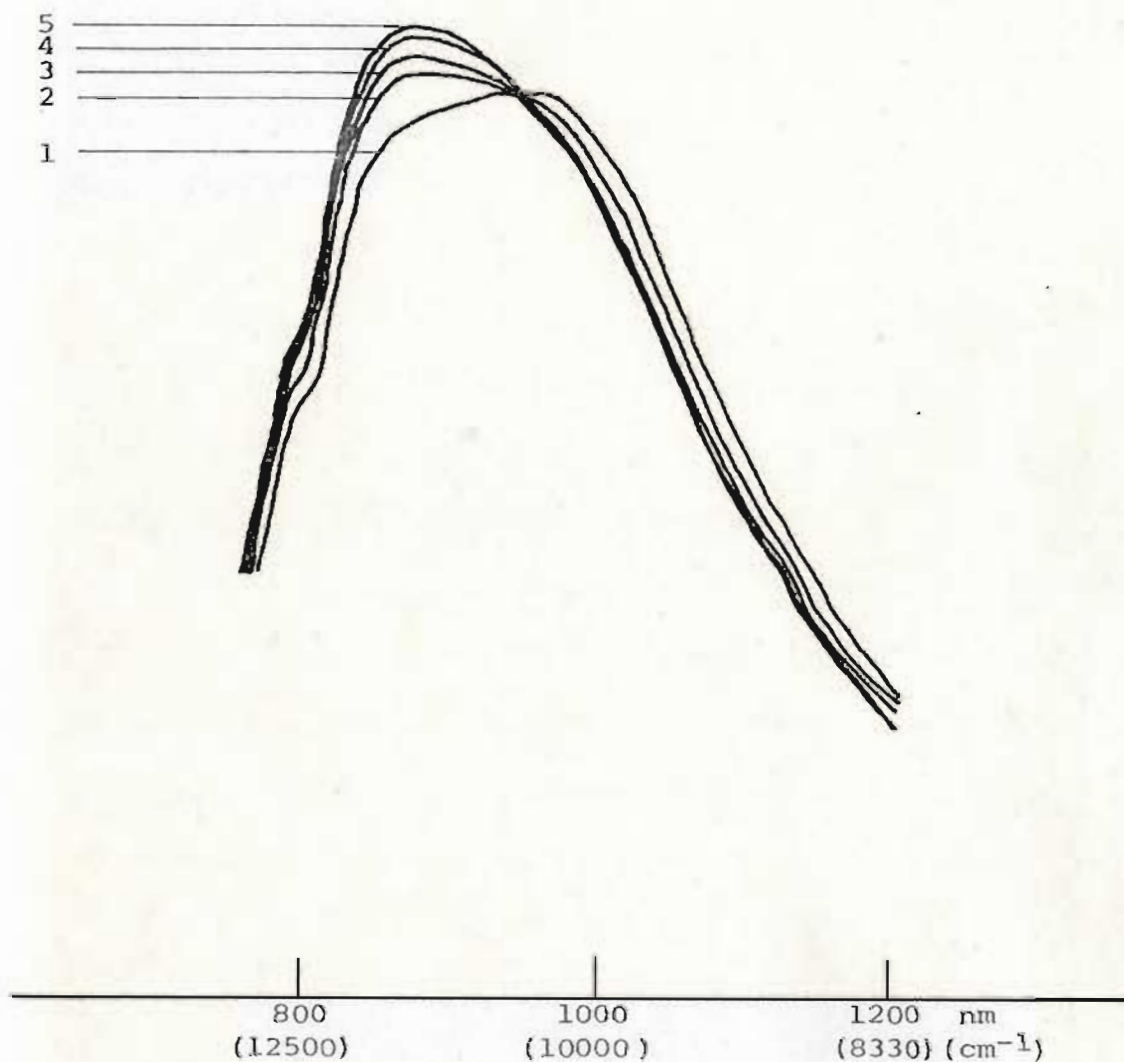
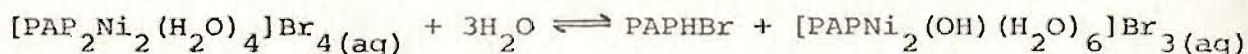


Fig.15

EFFECTS OF THE ADDITION OF conc.HCl ON  $\nu_1$   
OF  $[PAP_2Ni_2(H_2O)_4]Br_4(aq)$   
( 1 - NO HCl ; 2 → 5 - INCREASING HCl )

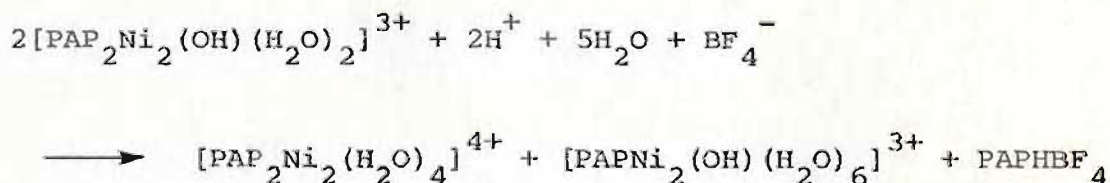
equilibrium consistent with these data is given below:



The species  $[\text{PAPNi}_2(\text{OH})(\text{H}_2\text{O})_6]\text{Br}_3$  postulated in the hydrolysis equilibrium may be responsible for the  $\nu_1$  absorption at  $10,300 \text{ cm}^{-1}$ .

The  $\nu_2$  absorption for this complex appears to be coincident with that of the tetraaquo complex.

Electronic spectra of solutions of the perchlorate and tetrafluoroborate complexes acidified with hydrochloric acid resemble that of the bromide complex in neutral solution, i.e. absorptions at  $10,300 \text{ cm}^{-1}$ ,  $11,500 \text{ cm}^{-1}$  and  $18,000 \text{ cm}^{-1}$ . The addition of acid causes a white precipitate to form in the solution of the tetrafluoroborate; infrared evidence indicates this precipitate to be a hydrotetrafluoroborate of PAP. Presumably the same reaction is occurring in the solutions of both the perchlorate and tetrafluoroborate complexes of PAP, but the PAP-hydroperchlorate is more soluble than the tetrafluoroborate analogue. The similarity of the electronic spectrum of the bromide complex to those of the perchlorate and tetrafluoroborate indicates the same species are in solution, one of which is the tetraaquo dimeric binuclear complex. Using the tetrafluoroborate as an example, the reaction of these two complexes may be as follows:



The charge transfer absorptions of the coordinated PAP of all the nickel complexes discussed here occur between  $28,500 \text{ cm}^{-1}$  and  $29,000 \text{ cm}^{-1}$  (Table 7). The charge transfer absorption for neutral PAP in a series of copper complexes has been reported to occur between  $27,400 \text{ cm}^{-1}$  and  $29,600 \text{ cm}^{-1}$ ; this suggests that the ligand is neutral in the nickel complexes.

TABLE 7

ELECTRONIC SPECTRAL DATA FOR THE PAP-NICKEL COMPLEXES<sup>a</sup>

COMPLEX	${}^3A_{2g} \rightarrow$	${}^3T_{2g}$	${}^1E_g$	${}^3T_{1g}(F)$	Dq	B	$\beta^b$	LIGAND CHARGE TRANSFER ( $\pi \rightarrow \pi^*$ )
$[PAP_2Ni_2(H_2O)_4]Cl_4$		11,500 [15]		18,200 [17]	1150	858	0.82	28,500 [30400]
$[PAP_2Ni_2(H_2O)_4]Br_4$		11,430 <sup>c</sup> [12]	15400 [5]	17,540 [12]	1143	714	0.70	28,800 [35000]
$[PAP_2Ni_2I_4]$		11,100 <sup>c</sup> [14]	15200 [7]	17,540 [15]	1110	822	0.82	28,600 [30900]
$[PAP_2Ni_2(OH)(NO_3)_3]$		12,120 <sup>c</sup> [8]		18,520 [8]	1212	739	0.71	28,600 [32200]
$[PAP_2Ni_2(NO_3)_4]$		11,430 <sup>c</sup> [6]		18,000 [5]	1143	828	0.80	28,600 [33200]
$[PAP_2Ni_2(OH)(H_2O)_2](ClO_4)_3$		11,430 <sup>c</sup> [15]		17,860 [12]	1143	788	0.76	29,000 [36000]
$[PAP_2Ni_2(OH)(H_2O)_2](BF_4)_3$		11,600 <sup>c</sup> [12]		17,700 [9]	1163	703	0.67	28,600 [36300]

<sup>a</sup> Band positions quoted in  $cm^{-1}$ . [ ] denotes extinction coefficient. Calculated positions of  $\nu_3$  of these complexes occur between 27,500 and 29,200  $cm^{-1}$ .

<sup>b</sup> Free ion value of B (B') for  $Ni^{2+} = 1040 cm^{-1}$ .

<sup>c</sup> This value represents a weighted average of the peaks in the absorption envelope.

MAGNETIC MEASUREMENTS

The magnetic susceptibility data for the compounds are given in Table 8. Diamagnetic corrections were made for the measured susceptibility of the ligand, and Pascal constants were used to correct for the magnetic effects of the anions and metal core electrons. A more detailed description of the treatment of the magnetic susceptibility data measured as a function of temperature is given in Appendix A.

TABLE 8

MAGNETIC PARAMETERS FOR THE PAP-NICKEL COMPLEXES

COMPOUND	$\mu_{\text{eff}}$ (295 K)	g	-J (cm <sup>-1</sup> )
[PAP <sub>2</sub> Ni <sub>2</sub> (H <sub>2</sub> O) <sub>4</sub> Cl <sub>4</sub> ]·3H <sub>2</sub> O	3.3	2.16	3.16
[PAP <sub>2</sub> Ni <sub>2</sub> (H <sub>2</sub> O) <sub>4</sub> ]Br <sub>4</sub>	3.3		
[PAP <sub>2</sub> Ni <sub>2</sub> I <sub>4</sub> ]	3.2		
[PAP <sub>2</sub> Ni <sub>2</sub> (OH)(NO <sub>3</sub> ) <sub>3</sub> ]	2.7		
[PAP <sub>2</sub> Ni <sub>2</sub> (NO <sub>3</sub> ) <sub>4</sub> ]	2.9		
[PAP <sub>2</sub> Ni <sub>2</sub> (OH)(H <sub>2</sub> O) <sub>2</sub> ](ClO <sub>4</sub> ) <sub>3</sub>	2.7	1.93	7.31
[PAP <sub>2</sub> Ni <sub>2</sub> (OH)(H <sub>2</sub> O) <sub>2</sub> ](BF <sub>4</sub> ) <sub>3</sub>	2.4		

As may be seen from the above table, the values of  $\mu_{\text{eff}}$  for the three halide complexes and that of the tetranitrate are in the range

characteristic of octahedrally coordinated nickel(II) (2.8 - 3.5 B.M.), while those of the other complexes lie below the spin-only value and suggest the possibility of antiferromagnetic exchange between the nickel atoms in these systems.

The value of  $J$  for the chloride complex suggests a weak antiferromagnetic interaction between the nickel atoms. In the case of the nickel(II) complexes of DHPH, DPPN etc.<sup>15</sup>, it has been proposed that such an exchange takes place via the  $\pi$ -system of the azine bridge.<sup>15</sup> The room temperature magnetic moments of the PAP-nickel bromide, iodide and tetranitrate complexes are higher than those of the binuclear DHPH and DPPN complexes, suggesting a weaker interaction between the metal atoms in the PAP complex, although this will have to be confirmed by further variable temperature susceptibility measurements. Although the room temperature magnetic moment of the nickel chloride complex of PAP is high, the  $J$  value of  $-3.16 \text{ cm}^{-1}$  suggests a weak antiferromagnetic exchange; this indicates a somewhat weaker interaction than is apparent in the complex  $\text{Ni}(\text{DHPH})\text{Cl}_2 \cdot 2\text{H}_2\text{O}$ . This difference can be rationalised in terms of a smaller degree of overlap between the metal orbitals and the  $\pi$ -orbitals of the azine bridge in the PAP complex. The geometry of the nickel chloride complex of DHPH allows the nickel atoms to lie in the same plane as the phthalazine rings, but such coplanarity is not allowed with PAP. The interposition of the exocyclic nitrogen atoms between the phthalazine and pyridine rings gives PAP more flexibility, with the formation of six-membered

metallated-rings. Molecular models indicate that the nickel octahedra are twisted about the nickel-phthalazine nitrogen bonds. This would probably result in reduced  $\pi$ -overlap between the azine  $\pi$ -orbitals and suitable metal orbitals and lead to a weaker exchange than that found in complexes of DHPH.

The room temperature magnetic moments of the hydroxy-nitrate, perchlorate and tetrafluoroborate complexes are lower than those of the other complexes, suggesting greater spin-spin exchange between the metal atoms. This is confirmed in the case of the perchlorate complex, which has a  $J$  value of  $-7.31 \text{ cm}^{-1}$ . Presumably the metal-ligand bonding does not vary greatly among the dimeric binuclear PAP-nickel complexes, so it is unlikely that the spin-spin interaction between the metal atoms of the hydroxy-nitrate, perchlorate and tetrafluoroborate complexes takes place via the azine bridge alone. The increased spin-spin coupling between the metal atoms in the perchlorate complex may be due to partial exchange via the hydroxy bridge.

The values of  $g$  and  $J$  quoted above are preliminary, determined from magnetic susceptibility studies over a narrow temperature range (ca.  $150^\circ\text{K} - 300^\circ\text{K}$ ). It is intended to repeat these studies over a wider range for a more accurate determination of these parameters.



### CONDUCTANCE DATA

The conductances of a series of aqueous solutions of each complex, ranging from  $10^{-3}$  to  $10^{-5}$  molar, were determined at  $25^{\circ}\text{C}$ . For each concentration a corrected conductance,  $L_{\text{CORR}}$ , was determined by subtracting the measured conductance of the water from that of the solution. The equivalent conductance,  $\Lambda_e$ , for each solution was calculated from the formula

$$\Lambda_e = 1000 K L_{\text{CORR}}/C_e$$

where  $K$  is the cell constant and  $C_e$  is the equivalent concentration of the electrolyte. For each complex, the limiting conductivity at infinite dilution,  $\Lambda_o$ , was calculated from a plot of  $\Lambda_e$  vs.  $\sqrt{C_e}$ . The slope,  $A$ , of the plot of  $\Lambda_o - \Lambda_e$  vs.  $\sqrt{C_e}$  is characteristic of the electrolyte type; a comparison of the experimental values of  $A$  with those of "standard" electrolytes may be used to determine the electrolyte type of the complex.

Values of  $A$  for standard electrolyte types in water are given in Table 9; the experimental values for the PAP-nickel complexes are given in Table 10.

As may be seen from the data in Table 10, the values of  $A$  confirm the assumed ion types for the chloride, nitrate and perchlorate complexes. This indicates that the species are completely hydrated in solution, even though they may contain coordinated anions in the solid state, as has been suggested in some cases.

TABLE 9

SLOPES OF  $(\Lambda_o - \Lambda_e)$  VS.  $\sqrt{C_e}$  FOR STANDARD ION TYPES IN WATER<sup>1</sup>

COMPOUND	ION TYPE	A
KCl	1:1	92
$[\text{Co}(\text{NO}_2)(\text{NH}_3)_5]\text{Cl}_2$	1:2	185
$\text{K}_3[\text{Fe}(\text{CN})_6]$	3:1	285
$\text{K}_4[\text{Fe}(\text{CN})_6]$	4:1	526

<sup>1</sup> These data are taken from a) The International Critical Tables, VOL. VI, The McGraw Hill Book Co., Inc., New York, 1929; and b) Handbuch der Anorganische Chemie, Kobalt B, Vol. 58, Verlag Chemie, Berlin, Germany, 1930.

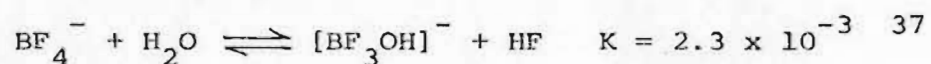
TABLE 10

SLOPES OF  $(\Lambda_o - \Lambda_e)$  VS.  $\sqrt{C_e}$  FOR PAP-NICKEL COMPLEXES IN AQUEOUS SOLUTIONS

COMPOUND	ASSUMED ION TYPE	A	$\Lambda_o$
$[\text{PAP}_2\text{Ni}_2(\text{H}_2\text{O})_4]\text{Cl}_4 \cdot 3\text{H}_2\text{O}$	1:4	527	121
$[\text{PAP}_2\text{Ni}_2(\text{H}_2\text{O})_4]\text{Br}_4$	1:4	1026	149
$[\text{PAP}_2\text{Ni}_2\text{I}_4]$	1:4	1232	156
$[\text{PAP}_2\text{Ni}_2(\text{OH})(\text{NO}_3)_3]$	1:3	234	107
$[\text{PAP}_2\text{Ni}_2(\text{NO}_3)_4]$	1:4	588	146
$[\text{PAP}_2\text{Ni}_2(\text{OH})(\text{H}_2\text{O})_2](\text{ClO}_4)_3$	1:3	325	135
$[\text{PAP}_2\text{Ni}_2(\text{OH})(\text{H}_2\text{O})_2](\text{BF}_4)_3$	1:3	1402	223

The values of A for the bromide, iodide and tetrafluoroborate complexes are anomalous. There was evidence that some HBr was formed in the nickel bromide - PAP reaction mixture (see experimental procedure). There is also evidence that in aqueous solution of the bromide complex an equilibrium exists which may produce HBr (see section on Electronic Spectra). If this is the case, it would account for the high slope (A) for the bromide complex. Presumably this could also be the case for the iodide complex.

The large value of A in the case of the tetrafluoroborate complex is probably due to hydrolysis of the tetrafluoroborate anion, producing HF and the hydroxofluoroborate ion



SUMMARY

Elemental analyses of the nickel halide complexes of PAP indicate that the empirical formulae are  $\text{PAPNiCl}_2 \cdot n\text{H}_2\text{O}$  ( $n = 1.5-3.5$ ),  $\text{PAPNiBr}_2 \cdot n\text{H}_2\text{O}$  ( $n = 1.5, 2$ ) and  $\text{PAPNiI}_2$ . The infrared spectra indicate that both pyridine rings of the ligand are coordinated. The infrared spectra are also similar to that of the binuclear compound  $\text{PAPCu}_2\text{Cl}_3(\text{OH})(\text{H}_2\text{O})$ , which has been characterised by x-ray analysis. The simplest structure consistent with all these data is a binuclear dimer having a molecular formula twice that of the empirical formula (Fig. 16). Molecular models indicate that such a structure is feasible, as the pyridine rings can twist to accommodate any repulsion that might arise between hydrogen atoms on adjacent rings. The magnetic moments of the solid state halide compounds are of the order 3.0 - 3.3 B.M., characteristic of octahedral and pseudo-octahedral nickel(II). Temperature dependent magnetic susceptibility studies of the chloride complex indicate there is a weak antiferromagnetic exchange taking place between the nickel atoms. The electronic spectra are consistent with "octahedral" complexes. Presumably, the chloride and bromide complexes contain coordinated water in the crystalline state; there is no infrared spectral evidence for Ni-X ( $X = \text{Cl}, \text{Br}$ ) stretching. (The solid iodide compound must contain coordinated iodine if the nickel atoms are to be in octahedral environments, although the electronic spectrum is not entirely consistent with this.) The conductance data for the chloride complex shows it is a 1:4 electrolyte in aqueous solution, which is consistent with the proposed structure.

The conductance data for the bromide and iodide complexes are not as readily interpreted as those of the chloride, the slopes of plots of  $(\Lambda_o - \Lambda_e)$  vs.  $\sqrt{C_e}$  being much higher than expected; this may be due to the presence of small amounts of acid. Despite the anomalous conductance data, the similarity of the infrared and electronic spectra of the three complexes indicate that the bromide and iodide complexes resemble the chloride.

The empirical formulae of the tetrafluoroborate and perchlorate complexes are indicated by elemental analyses to be  $\text{PAP}_2\text{Ni}_2\text{Y}_3 \cdot 3\text{H}_2\text{O}$ . The infrared spectra of these two complexes are quite similar, apart from anion absorptions, so it is assumed these compounds are isostructural. Infrared evidence indicates the perchlorate ion is not coordinated, and since the tetrafluoroborate ion does not coordinate, these complexes must contain coordinated water. The electronic spectra of these two complexes indicate the nickel atoms are in octahedral environments. This condition may be satisfied if one of the coordinated "waters" represents a bridging hydroxide, which would also balance the electric charges. The magnetic susceptibilities of the perchlorate and tetrafluoroborate complexes are 2.7 and 2.4 B.M. respectively, low enough to indicate some form of magnetic interaction between the nickel atoms, as is confirmed by a  $J$  value of  $-7.31 \text{ cm}^{-1}$  for the perchlorate complex. Although the role of the hydroxide bridge in such magnetic interactions is not clear, it may bring the nickel atoms close enough for some direct interaction, or may itself provide a

pathway for indirect interaction. Interaction may also take place via the nitrogen atoms of the azine bridge (see Fig. 17).

The conductivity study of the perchlorate complex indicates it is a 1:3 electrolyte, which is consistent with the proposed formula. The unexpectedly high conductivity of the tetrafluoroborate complex is attributed to hydrolysis of the tetrafluoroborate anion.

The two nitrate complexes  $\text{PAP}_2\text{Ni}_2(\text{NO}_3)_4$  and  $\text{PAP}_2\text{Ni}_2(\text{OH})(\text{NO}_3)_3$  have been shown to be 1:4 and 1:3 electrolytes respectively, indicating the nitrate groups to be labile. Although the infrared evidence is inconclusive, the nickel atoms must have nitrate groups coordinated to them to complete the octahedral environments indicated by the solid state electronic spectra. The low magnetic moment of the trinitrate may be due to spin-spin exchange between the nickel atoms. The two metal atoms may be held close enough for metal-metal interaction via a bridging nitrate group, or such interaction may take place through the hydroxy bridge and/or the ligand azine bridge.

Aside: In an attempt to produce a hydroxy bridged species from the chloride complex, potassium hydroxide solution was added to an aqueous solution of  $[\text{PAP}_2\text{Ni}_2(\text{H}_2\text{O})_4]\text{Cl}_4$ . The addition of a small amount of base caused a yellow precipitate to form. The electronic spectrum of the remaining solution was essentially the same as that of the dissolved chloro complex, indicating no great change in the nickel chromophore. Further studies indicate that the yellow precipitate formed by the addition of base is soluble in chloroform. It is known that  $\text{PAPCu}_2\text{Cl}_3(\text{OH})(\text{H}_2\text{O})$  reacts with base to produce a neutral species

$\text{PAP}_2\text{Cu}$  which is soluble in chloroform<sup>2</sup>. By analogy, it is assumed that a similar species is produced with the nickel system. Further studies on systems of this type are underway but will not be reported here.

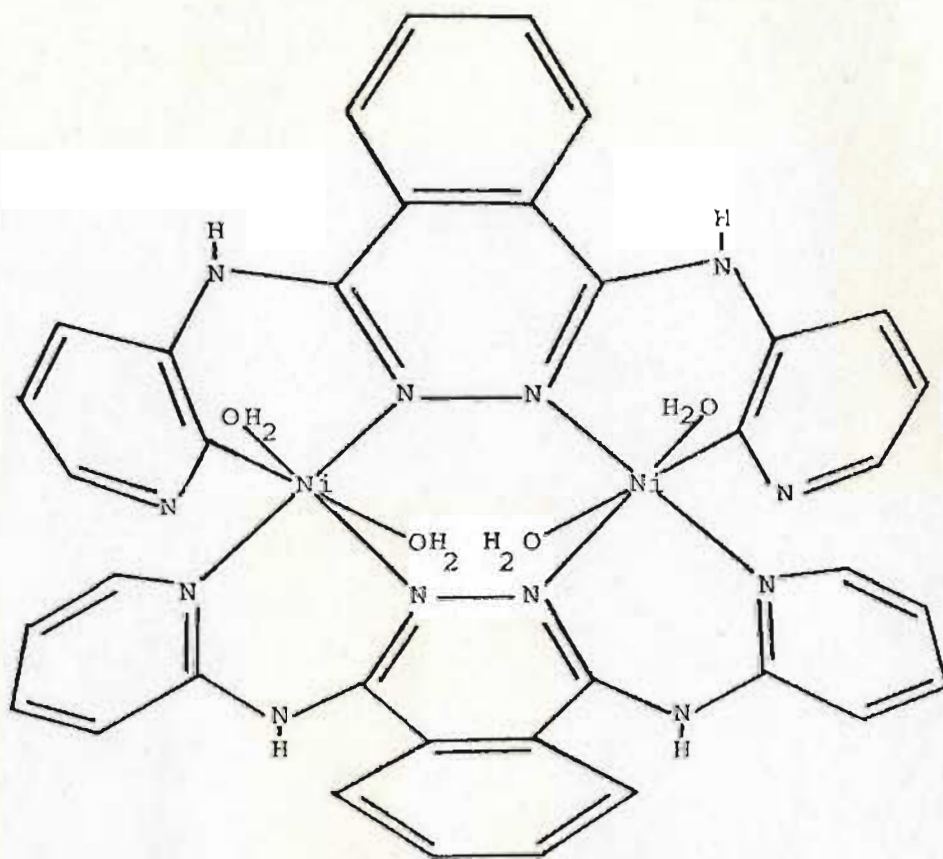


Fig. 16

A PROPOSED STRUCTURE FOR THE CATION IN THE  
COMPLEX  $[PAP_2 Ni_2 (H_2O)_4] Cl_4$ .



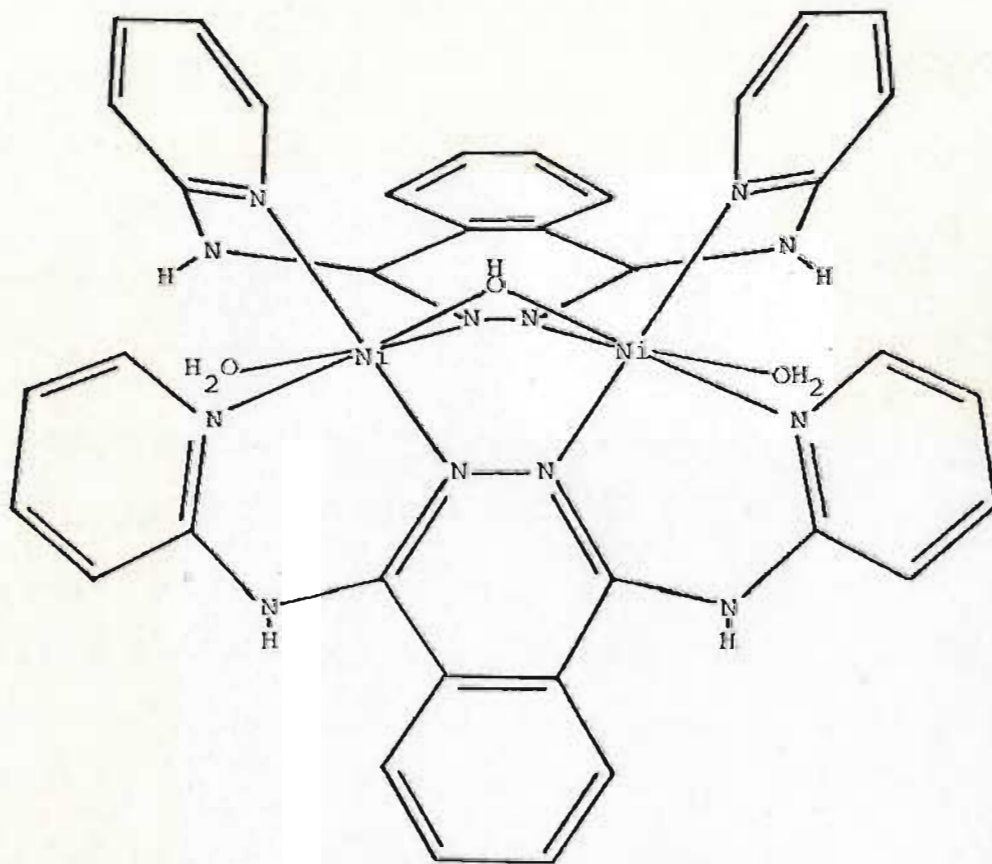


Fig. 17

A PROPOSED STRUCTURE FOR THE CATION IN THE  
COMPLEX  $[PAP_2Ni_2(OH)(H_2O)_2] (ClO_4)_3$ .

### ZINC(II) COMPLEXES OF PAP

The study of the chelating properties of PAP was extended to the preparation of several zinc complexes. These complexes were prepared in ethanol by adding a hot solution of the ligand to a solution of the zinc salt; the products were obtained as cream or yellow precipitates. The complexes are insoluble in water and common organic solvents, although they show some solubility in dimethylsulphoxide (DMSO). The compounds are decomplexed in pyridine; the chloride complex when dissolved in pyridine, yields a white crystalline solid, which infrared evidence indicates to be  $(\text{pyridine})_2 \text{ZnCl}_2$ .

#### INFRARED SPECTRAL DATA

Assignments of ligand absorptions in these complexes are shown in Table 11. The bromide and iodide complexes show two pyridine ring breathing mode absorptions, occurring near  $1015 \text{ cm}^{-1}$  and  $990 \text{ cm}^{-1}$ . These two absorptions imply the presence of coordinated and uncoordinated pyridine rings in the ligand. These data, combined with the results of elemental analyses indicate the complexes to be mononuclear, presumably containing bidentate PAP. The single ring breathing mode absorption of the chloride complex, found at  $1010 \text{ cm}^{-1}$ , indicates the ligand is coordinating via both pyridine rings; for this to be consistent with the results of the elemental analyses, the chloride complex must be binuclear and dimeric. That the complex of the chloride is binuclear, whereas those of the bromide and iodide are mononuclear is probably related to the relative sizes of the co-

ordinated halides. All three complexes show a strong, sharp band at  $3360\text{ cm}^{-1}$ , assigned to exocyclic N-H stretch. Absorptions occurring in the region  $3300\text{--}3000\text{ cm}^{-1}$  are assigned to N-H stretching (see Table 11). The low energy region of the infrared spectrum of the chloride complex contains unique absorptions at  $305\text{ cm}^{-1}$  and  $330\text{ cm}^{-1}$ . These bands are assigned to Zn-Cl stretching vibrations by analogy with  $(\text{pyridine})_2\text{ZnCl}_2$ , which shows Zn-Cl absorptions at  $296\text{ cm}^{-1}$  and  $329\text{ cm}^{-1}$ .<sup>38</sup> The presence of two bands attributable to Zn-Cl stretching implies a "cis" arrangement of donor atoms around the zinc centre, and since the complex is binuclear and dimeric, a "cis"-octahedral structure with no bridging group other than phthalazine is proposed. An absorption occurring at  $238\text{ cm}^{-1}$  in the spectrum of the bromide complex has been assigned to Zn-Br stretching, as this occurs in the same area as the Zn-Br stretching vibrations of  $(\text{phthalazine})_2\text{ZnBr}_2$  (i.e.,  $232\text{ cm}^{-1}$  and  $246\text{ cm}^{-1}$ ).<sup>38</sup> The single metal-halide absorption gives little structural information, but if the complex is monomeric, steric requirements would probably favour a tetrahedral field around the zinc atom. If the zinc is coordinated in a tetrahedral manner, the second Zn-Br stretching vibration may be hidden by ligand absorptions, or the two bands expected may remain unresolved in the same band envelope.

The spectrum of the thiocyanate complex shows a single pyridine ring breathing mode absorption around  $1010\text{ cm}^{-1}$  (Table 11), indicating the coordination of both ligand pyridine rings. An intense single absorption occurring at  $2060\text{ cm}^{-1}$  has been assigned to CN stretching

TABLE 11

## INFRARED SPECTRAL DATA FOR ZINC COMPLEXES OF PAP

COMPOUND	$\nu_{\text{H}_2\text{O}}$ ( $\text{cm}^{-1}$ )	$\nu_{\text{N-H}}$ ( $\text{cm}^{-1}$ )	$\nu_{\text{C-H}}$ ( $\text{cm}^{-1}$ )	PYRIDINE RING ( $\text{cm}^{-1}$ ) BREATHING MODE	$\nu_{\text{Zn-X}}$ ( $\text{cm}^{-1}$ )
[PAP <sub>2</sub> Zn <sub>2</sub> Cl <sub>4</sub> ]		3360 (st.,sh.) 3220 (wk.)	3140 (wk.) 3080 (wk.) 3060 (wk.)	1010 (m.st.,sh.)	330 (m.st.) 305 (m.st.)
[PAPZnBr <sub>2</sub> ]·H <sub>2</sub> O	3440 (wk.)	3360 (st.,sh.) 3250 (wk.) 3220 (wk.)	3180 (wk.) 3140 (wk.) 3120 (wk.) 3060 (wk.) 3040 (wk.)	1018 (m.st.,sh.) 990 (st.,sh.)	238 (wk.)
[PAPZnI <sub>2</sub> ]·H <sub>2</sub> O	3440 (wk.)	3360 (st.,sh.) 3220 (wk.)	3180 (wk.) 3140 (wk.) 3060 (wk.) 3040 (wk.)	1015 (m.st.,sh.) 990 (st.,sh.)	-
[PAP <sub>2</sub> Zn <sub>2</sub> (SCN) <sub>4</sub> ] ·H <sub>2</sub> O	-	3300 (m.st.,br.) 3220 (wk.)	3160 (wk.) 3130 (wk.) 3080 (wk.)	1010 (m.st.)	-

m.st., medium strong; st., strong; sh., sharp; wk., weak

in a thiocyanate group terminally bonded by the nitrogen atom. Other infrared absorptions expected to arise from the thiocyanate group are masked by ligand absorptions. The elemental analyses of the complex indicates the metal to ligand ratio is 1:1, which, to be consistent with the infrared spectrum, means that the complex is binuclear and dimeric, and probably has a "trans"-octahedral structure.

#### NUCLEAR MAGNETIC RESONANCE SPECTRAL DATA

To further characterize the compounds NMR spectra of PAP, the zinc-chloride, -bromide, and -thiocyanate complexes were determined in deuterated DMSO. The resonance peaks associated with the ligand were assigned by comparing the spectrum of PAP (Fig. 18) with the spectra of phthalazine and 2-aminopyridine, and also by carrying out spin decoupling experiments. The assigned chemical shifts of the protons in PAP are shown in Table 12, which also includes the chemical shifts of the relevant protons of phthalazine and 2-aminopyridine. Spin decoupling studies of PAP show that there is coupling between the protons resonating at 7.31, 8.09 and 8.66 ppm; these are therefore assigned to the pyridine hydrogens. Likewise, evidence of coupling between the protons giving rise to the multiplets occurring at 8.28 and 8.84 ppm indicates these protons belong to the phthalazine moiety of the ligand. If the phthalazine hydrogens belong to an AA'BB' system, then their resonance peaks would be mirror images of each other, which is not the case here. The asymmetry of these two sets of peaks may arise from a rapid exchange in solution between the three tautomeric forms of PAP, or it may indicate that a

large proportion of the PAP in solution exists in the form having one hydrogen on an exocyclic amino group and one on a phthalazine nitrogen (see Fig. 2), thereby reducing the symmetry of the system.

The addition of trifluoroacetic acid (TFA) to the solution of PAP in DMSO- $d_6$  enhanced the resolution of the spectrum, as well as causing shifts in the resonant frequencies of some of the protons (see Table 12, and Fig. 19). The acid presumably protonates all available nitrogen atoms and prevents changes in the tautomeric form of the dissolved ligand. That the presence of acid does have such an effect is an indication that the ligand is not necessarily in a single tautomeric form in the DMSO solution. There is an overlap of the absorptions of the  $H_{3,3'}$ ,  $H_{4,4'}$ , and  $H_{6,6'}$  protons, resulting in a complex multiplet centered around 8 ppm. The addition of the TFA also causes the  $H_{2,2'}$  protons to appear as a triplet of doublets, as is the case with the spectra of the zinc bromide and thiocyanate complexes of PAP. The implications of this similarity in the pattern of the  $H_{2,2'}$  proton resonances in the acidified PAP and the bromide and thiocyanate complexes on the conformation of the ligand bears further study.

Except for minor changes in the chemical shifts, the NMR spectra of the zinc complexes are very similar to that of the uncoordinated ligand (see Figs. 18, 20, 21). The spectra of the complexes indicate that both pyridine rings of the ligand are equivalent, which is at first unexpected in the case of the bromide complex, since infrared evidence indicates it to be mononuclear. Electronic spectra confirm

that a change takes place when the complexes are dissolved in DMSO. The free ligand, when dissolved in methanol or DMSO has a charge transfer absorption occurring near  $27,400 \text{ cm}^{-1}$ . For the zinc complexes dissolved in methanol this absorption occurs around  $28,800 \text{ cm}^{-1}$ , but when they are dissolved in DMSO, this band occurs at ca.  $27,500 \text{ cm}^{-1}$ . Although the electronic spectra clearly indicate a change does occur when the complexes are dissolved in DMSO, this change may not necessarily involve complete decomplexation of the compound, as the proton chemical shifts of the complexes in DMSO differ from those of the free ligand. It is possible that in DMSO solution all the zinc complexes are binuclear, but with coordination taking place only via the phthalazine nitrogens. This would leave the pyridine rings free, and magnetically equivalent, and would also maintain a  $C_2$  axis through the ligand, explaining why the phthalazine proton absorptions are more symmetric in the NMR spectra of the complexes than they are in the free ligand. A sample of the chloride complex recrystallized from DMSO formed yellow crystals, which, after vacuum drying, showed infrared absorptions due to the ligand and DMSO. Absorptions between  $900-1100 \text{ cm}^{-1}$  due to both PAP and DMSO make it very difficult to determine from infrared evidence the manner of coordination between the zinc and the PAP, however it is assumed that DMSO itself is coordinated to the metal atom. Due to the fact that there was only a very small amount of this compound, a complete characterization was not achieved.

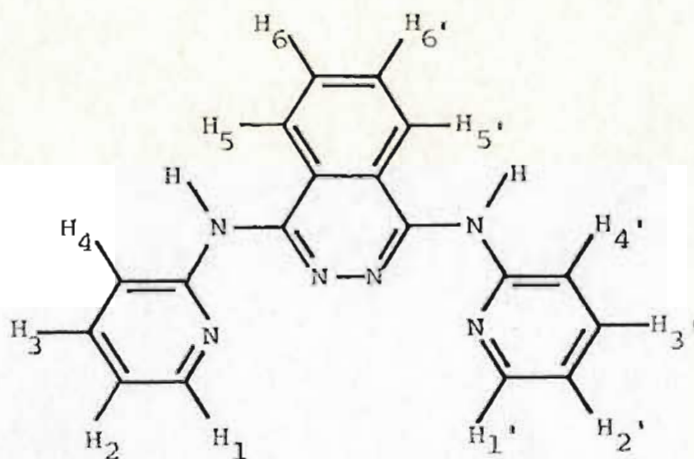


TABLE 12

CHEMICAL SHIFTS OF THE PROTONS OF PAP AND SOME ZINC COMPLEXES.

(CHEMICAL SHIFTS IN PPM)

(TEMPERATURES OF SOLUTIONS 334-347 K)

	H <sub>1,1'</sub>	H <sub>2,2'</sub>	H <sub>3,3'</sub>	H <sub>4,4'</sub>	H <sub>5,5'</sub>	H <sub>6,6'</sub>
PAP	8.66 <sup>c</sup>	7.31 <sup>d</sup>	8.06 <sup>e</sup>	8.06 <sup>e</sup>	8.84 <sup>d</sup>	8.28 <sup>d</sup>
PAP + TFA	8.39 <sup>c</sup>	7.31 <sup>f</sup>	ca.8 <sup>e</sup>	ca.8 <sup>e</sup>	8.82 <sup>g</sup>	8.13 <sup>d</sup>
PAP <sub>2</sub> Zn <sub>2</sub> Cl <sub>4</sub>	8.65 <sup>c</sup>	7.40 <sup>d</sup>	8.19 <sup>e</sup>	8.19 <sup>e</sup>	8.97 <sup>d</sup>	8.37 <sup>d</sup>
PAPZnBr <sub>2</sub> ·2H <sub>2</sub> O	8.35 <sup>c</sup>	7.16 <sup>f</sup>	7.88 <sup>e</sup>	7.88 <sup>e</sup>	8.74 <sup>d</sup>	8.13 <sup>d</sup>
PAP <sub>2</sub> Zn <sub>2</sub> (SCN) <sub>4</sub> ·2H <sub>2</sub> O	8.57 <sup>c</sup>	7.29 <sup>f</sup>	8.02 <sup>c</sup>	8.08 <sup>c</sup>	8.90 <sup>d</sup>	8.29 <sup>d</sup>
2-AMINOPYRIDINE <sup>a</sup> (IN DMSO)	8.11	6.60	7.44	7.70	-	-
PHTHALAZINE <sup>b</sup> (IN ACETONE)	-	-	-	-	8.13	8.01

a) Source: W. Brugel; Z. Electrochem., 66, 159 (1962)

b) Source: P.J. Black, M.L. Heffernan; Aust. J. Chem. 18, 707 (1965)

c) Doublet (with evidence of some long range coupling)

d) Multiplet

e) The overlap of this absorption with an adjacent absorption does not allow a definite assignment

f) Triplet of doublets

g) Determined from J<sub>5,6</sub> and position of first line in absorption group.



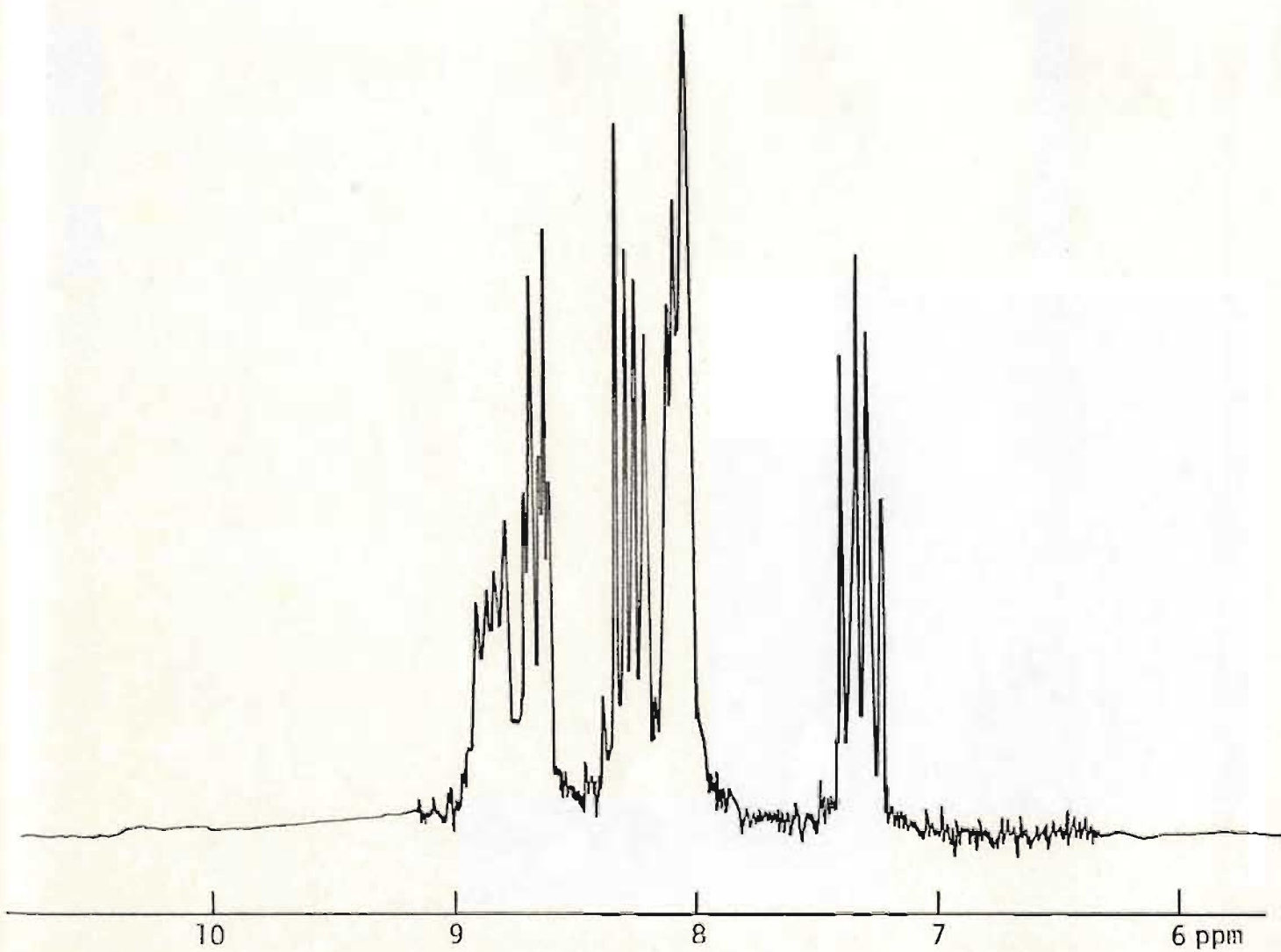


Fig.18

NMR SPECTRUM OF PAP IN DMSO.

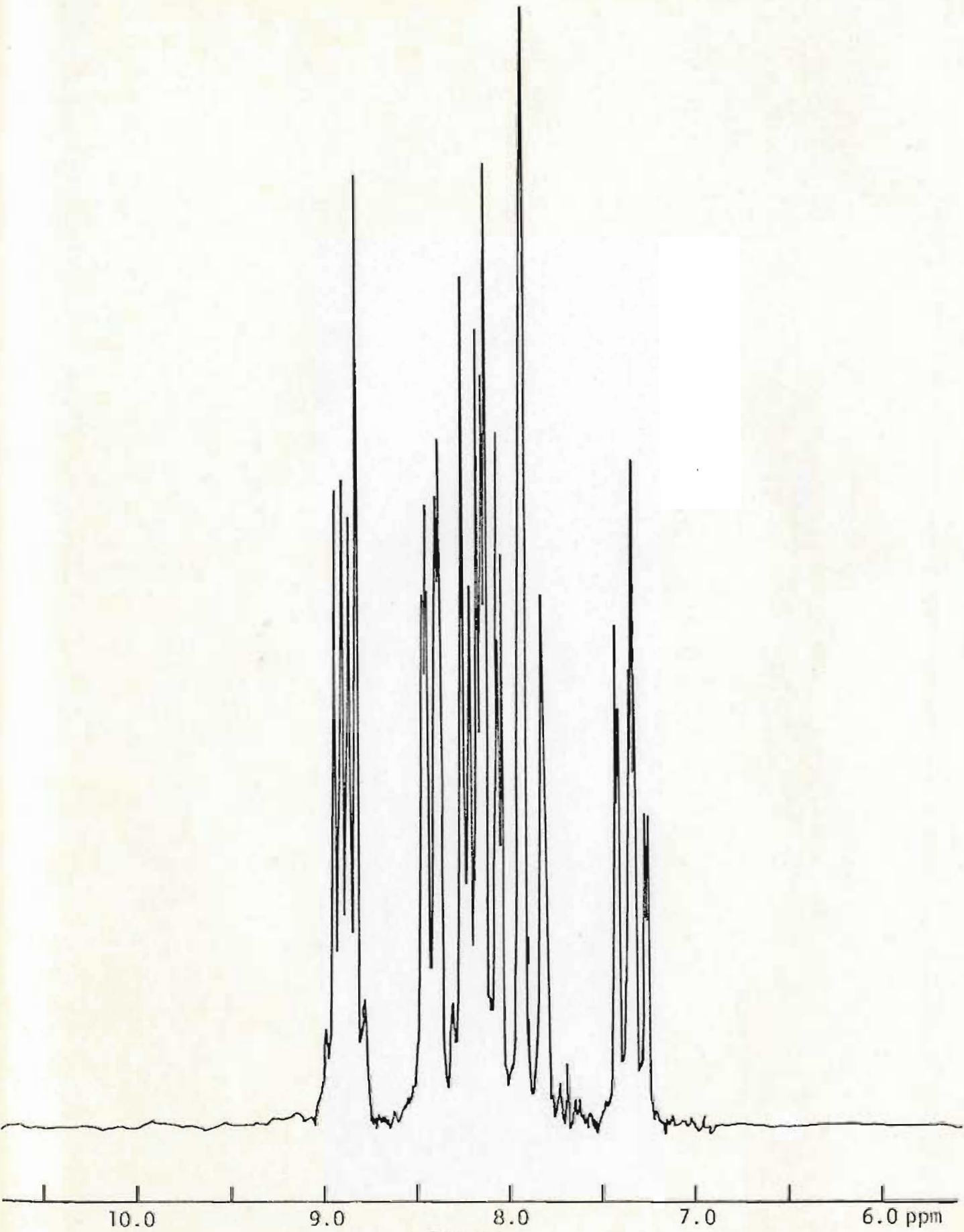


Fig.19

NMR SPECTRUM OF PAP IN DMSO WITH TRIFLUOROACETIC ACID ADDED.

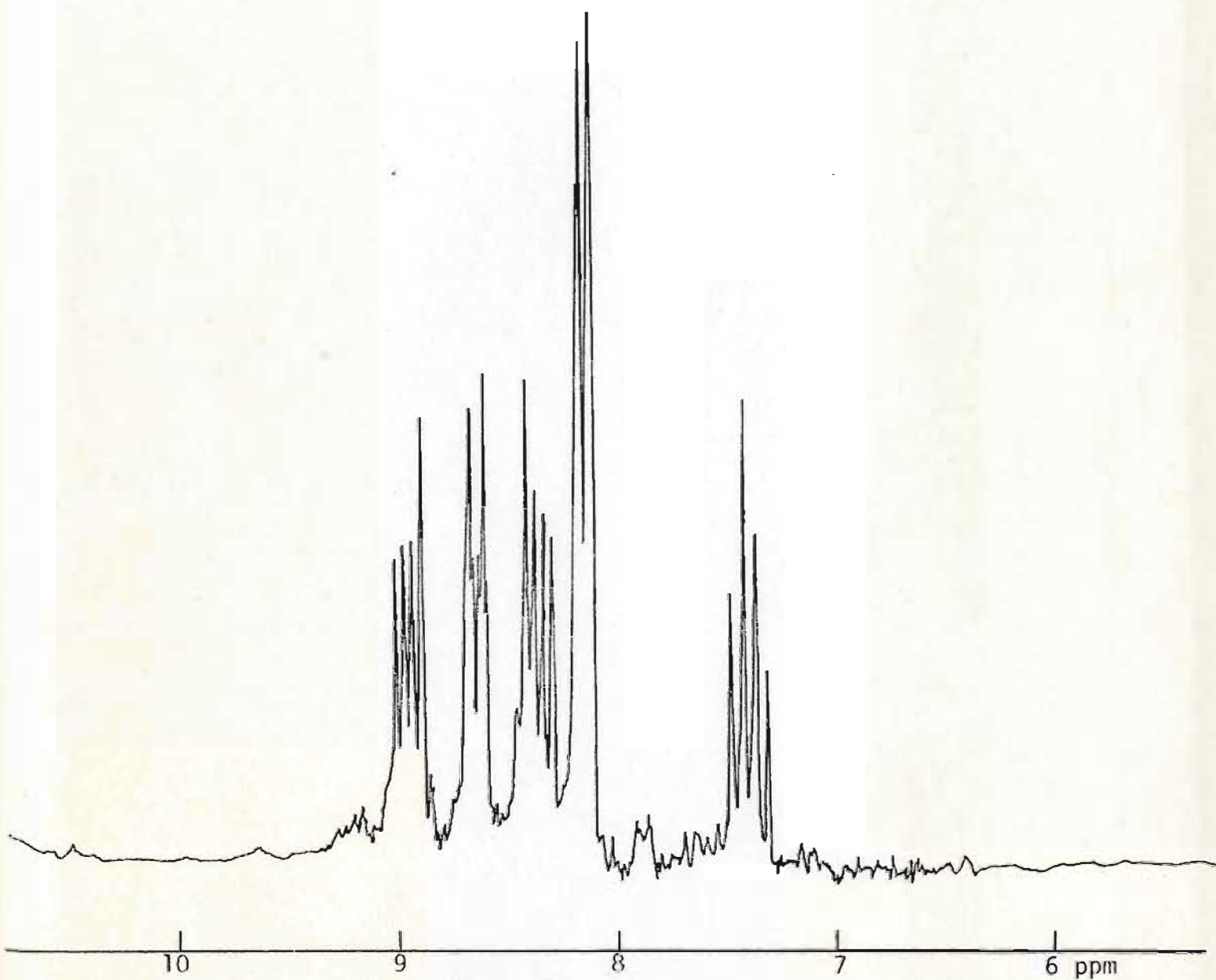


Fig. 20

NMR SPECTRUM OF PAP-ZINC CHLORIDE COMPLEX IN DMSO.

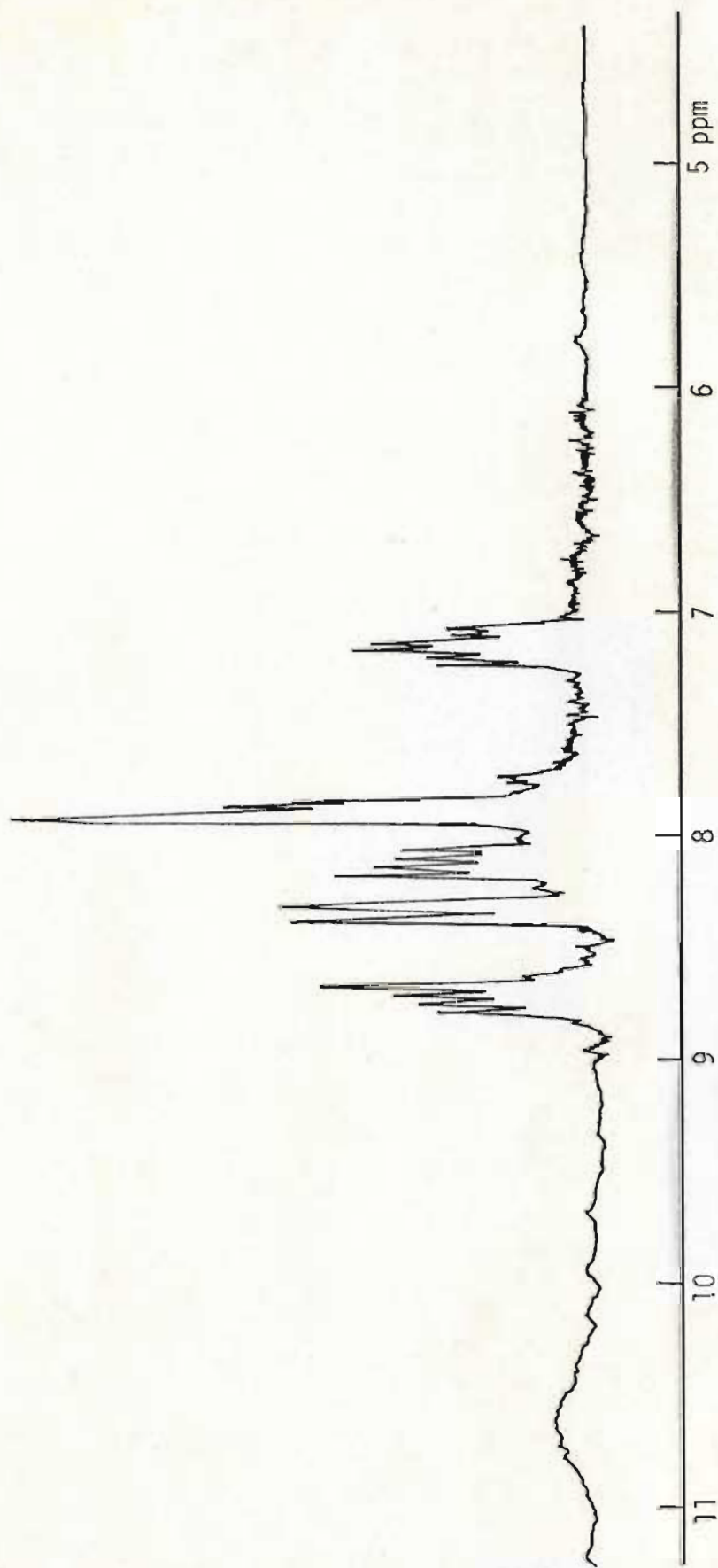


Fig. 21

NMR SPECTRUM OF PAP-ZINC BROMIDE COMPLEX IN DMSO.

## EXPERIMENTAL

The C,H,N analyses were carried out by Atlantic Microlab, Inc., Atlanta, Georgia. The metal analyses for the nickel complexes were done by first digesting the sample in ternary solution (10 parts conc.  $\text{HNO}_3$ :1 part conc.  $\text{H}_2\text{SO}_4$ :4 parts 70%  $\text{HClO}_4$ ) diluting to volume and then determining the nickel concentration by atomic absorbance. The zinc complexes were analysed by digesting the compound in concentrated nitric acid, diluting to volume and measuring the zinc content by atomic absorbance.

### Infrared Spectroscopy

All infrared spectra were determined on a Perkin-Elmer model 283 spectrophotometer as solid mulls. Potassium bromide plates were used in the region  $4000 - 600 \text{ cm}^{-1}$  and cesium iodide plates in the region  $600 - 200 \text{ cm}^{-1}$ . The mulling agents used were Nujol in the regions  $4000 - 3200 \text{ cm}^{-1}$ ,  $2700 - 1500 \text{ cm}^{-1}$ ,  $1300 - 200 \text{ cm}^{-1}$ , and hexachlorobutadiene in the regions  $4000 - 2700 \text{ cm}^{-1}$  and  $1500 - 1300 \text{ cm}^{-1}$ . The pyridine ring breathing mode absorptions were checked against calibrated absorptions of polystyrene.

### Electronic Spectroscopy

Electronic spectra of both solids and solutions were obtained using a Cary 17 spectrophotometer. The solid spectra were run as moderately strong mulls in nujol, which were spread onto filter paper and held between glass microscope slides. A blank of nujol was prepared in the same manner. The solid state spectra were determined from

1800 nm - 400 nm ( $5550 \text{ cm}^{-1}$  -  $20,000 \text{ cm}^{-1}$ ). Solution spectra were determined from 1200 nm - 200 nm ( $8300 \text{ cm}^{-1}$  -  $40,000 \text{ cm}^{-1}$ ). Scanning below  $8300 \text{ cm}^{-1}$  was not possible because of water absorptions.

#### Magnetic Susceptibility Studies

The room temperature magnetic susceptibilities were determined by the Faraday method using a Cahn Model 7600 electrobalance. The calibrant used was mercury tetrathiocyanatocobaltate(II). The molar susceptibilities were corrected for the measured diamagnetism of the ligand while Pascal's constants were used to correct for the diamagnetic contributions of water (if any), anions, and the metal core electrons. The magnetic moments were calculated using the formula:

$$\mu_{\text{eff}} = 2.828 (0.5 \chi_{\text{M}}^{\text{CORR}} T)^{1/2}$$

where  $0.5 \chi_{\text{M}}^{\text{CORR}}$  is used since there are two moles of nickel atoms per mole of complex.

The temperature dependent magnetic susceptibilities were determined with a Gouy magnetic balance fitted with a cyrostat. The magnetic balance consists of a Varian 4-inch electromagnet, Model V 4084, with two inch tapered pole caps, used in conjunction with a Spoerhaese Model 10 M microbalance with a sensitivity of  $\pm 0.01$  mg. A Varian model U 2300 A power supply and Model 2301 A current regulator are used to control the current. The cyrostat used for the temperature control is shown in Figure 21 (see also Appendix A). This apparatus has been described in the literature by Clark and O'Brien<sup>39</sup>. Mercury tetrathiocyanatocobaltate(II) was used as the calibrant.

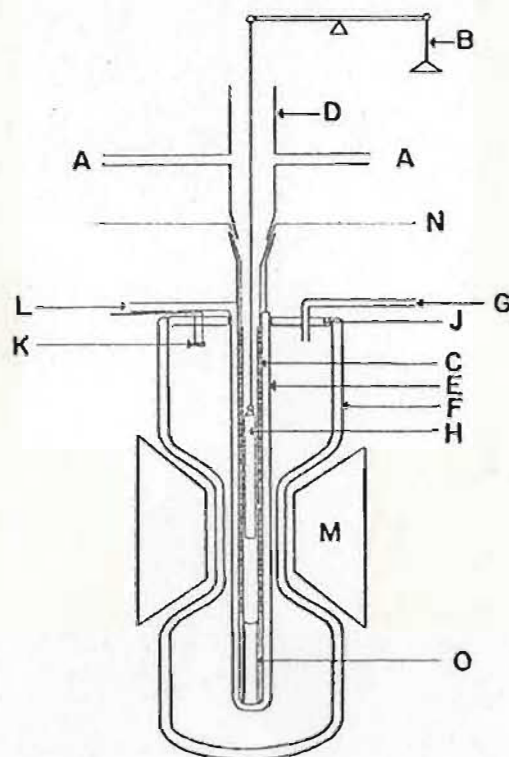


FIG. 1. Cryostat for the magnetic balance. A, nitrogen gas inlet and outlet; B, balance; C, heater and platinum resistance thermometer wound on brass former; D, draught shield; E, inner Dewar; F, outer Dewar; G, liquid nitrogen inlet; H, sample tube; J, icing shield; K, thermistor; L, to the pump for evacuation of the inner Dewar; M, magnet pole caps; N, connection to the heater and resistance thermometer; O, support for heater former.

FIGURE 22  
(see Ref. 39)

### Conductivity Measurements

Concentration dependent conductivity studies were carried out in aqueous solution using a general Radio Company bridge with impedance comparator and a constant temperature bath adjusted to 25°C. The conductivity of each complex was studied over a concentration range of  $10^{-3}$  M to  $10^{-5}$  M. The slopes and intercepts of the plots were determined using linear regression analysis.

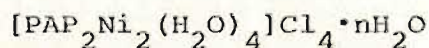
### PREPARATIVE PROCEDURES

#### PREPARATION OF THE LIGAND 1,4-DI(2'-PYRIDYL)AMINOPHTHALAZINE (PAP)

A mixture of o-phthalonitrile (16 g, 125 mmoles) and 2-aminopyridine (23.7 g, 252 mmoles) was prepared by grinding the two together in a mortar. This mixture was put in a 250 ml beaker and fused at 250° for approximately eight hours. As the reaction progressed, any sublimed material which formed on the sides of the beaker or the watch-glass cover was scraped back into the reaction solution. The cooled crude product was crushed and purified by crystallisation from ethanol. The purified PII (refer to Introduction) was dissolved in boiling ethanol and hydrazine hydrate (8 ml. of 85% solution, 136 mmoles) was added to the hot solution. The PAP so formed from the ring expansion reaction was allowed to crystallise out overnight as large yellow crystals.

YIELD: 27 g (70%); m.p. 211-13° (lit. 210°)

#### PREPARATION OF THE PAP-METAL COMPLEXES



PAP (1.50 g, 4.77 mmoles) was added to a solution of  $\text{NiCl}_2 \cdot 6\text{H}_2\text{O}$  (1.13 g, 4.75 mmoles) in 50 ml distilled water, and the mixture heated gently while being stirred. The PAP eventually reacted with the nickel salt to produce a clear solution which was purple by reflected light but dark blue by transmitted light. The solution was filtered and the volume reduced. The product came out as either dark purple crystals or a green powder. These appear to be different hydrated forms, because both have the same infrared spectrum, and the green powder redissolved to form a purple solution. The product was



recrystallised from water, and dried for three hours at 80° and 0.05 mm Hg. It was found that different hydrated forms were obtained if the temperature or length of drying time was varied.

YIELD: 1.76 g (77%)

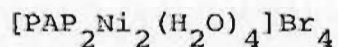
ANALYSES

$[\text{PAP}_2\text{Ni}_2(\text{H}_2\text{O})_4]\text{Cl}_4 \cdot 3\text{H}_2\text{O}$  FOUND C 42.67% H 3.34% N 16.60% Ni 12.30%

REQ. C 42.64% H 4.17% N 16.58% Ni 11.58%

$[\text{PAP}_2\text{Ni}_2(\text{H}_2\text{O})_2\text{Cl}_2]\text{Cl}_2$  FOUND C 46.54% H 3.53% N 18.11% Ni 12.75%

REQ. C 46.80% H 3.49% N 18.19% Ni 12.71%

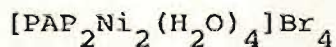


The same procedure was followed as that described for the preparation of  $[\text{PAP}_2\text{Ni}_2(\text{H}_2\text{O})_4]\text{Cl}_4 \cdot n\text{H}_2\text{O}$ , using 1.50 g PAP (4.77 mmoles) and 1.30 g  $\text{NiBr}_2 \cdot 3\text{H}_2\text{O}$  (4.77 mmoles). The solution of the complex was dark blue in colour, and as with the chloride complex, the bromide also formed blue crystals or a green powder, the two representing different hydrated forms. It was found that along with the purple crystals and green powder, aggregates of needle-like white crystals formed, especially if the solution was allowed to sit for a long time. The infrared spectrum of this compound resembled that of PAP. Although the pyridine ring breathing mode absorption of this substance was weaker than that of PAP, it indicated that the pyridine rings are uncoordinated. These white crystals form a yellow solution which gives a cream coloured precipitate in the presence of  $\text{Ag}^+$ . It is known that the ligand forms acid salts which are colourless but form

yellow solutions; presumably these white crystals are a hydrobromide salt of PAP. The PAP-nickel bromide complex was recrystallised from water and dried for three hours at 80° and 0.05 mm Hg.

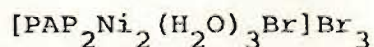
YIELD: 1.89 g (69%)

ANALYSES



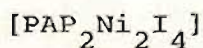
FOUND C 37.52% H 2.98% N 14.74%

REQ. C 38.00% H 3.19% N 14.77%



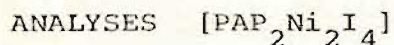
FOUND C 38.70% H 2.66% N 15.08% Ni 10.69%

REQ. C 38.62% H 3.06% N 15.01% Ni 10.49%



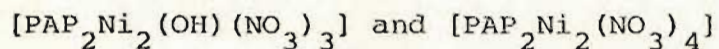
The preparative procedure for this compound is the same as that of the chloride complex. Since the purity of the nickel iodide was questionable an excess of  $\text{NiI}_2$  was reacted with the 1.50 g PAP. A grey-green amorphous precipitate formed as the reaction progressed, and the reaction mixture was boiled for one hour to ensure that all of the ligand had reacted. The mixture was filtered and the purple filtrate reduced in volume. The product came out of solution as dark green crystals. The product was recrystallised from water. After being dried under vacuum (at 80° and 0.05 mm Hg for 3 hrs) the product turned green-brown.

YIELD: 0.53 g (18%)



FOUND C 34.86% H 2.58% N 13.69%

REQ. C 34.49% H 2.25% N 13.41%



The same procedure was followed as that described for the preparation of  $[\text{PAP}_2\text{Ni}_2(\text{H}_2\text{O})_4]\text{Cl}_4 \cdot n\text{H}_2\text{O}$  using 1.50 g PAP (4.77 mmoles) and 1.43 g of  $\text{Ni}(\text{NO}_3)_2 \cdot 6\text{H}_2\text{O}$  (4.92 mmoles). After completion of the reaction, the colour of the solution was dark green. The solution was reduced in volume and allowed to crystallise slowly at room temperature (ca. 22°). The first two crystal crops were long, needle-like purple crystals, which were shown to be the hydroxy nitrate complex. Subsequent preparations of the nitrate complexes indicated the yield of the hydroxy nitrate complex improved if an excess of PAP was used, and the unreacted ligand filtered off before crystallisation. After drying the hydroxy nitrate crystals turned grey, but redissolved to form a purple solution. Attempts to recrystallise the hydroxy nitrate from water indicated the complex gradually changed in solution to a green compound. Further crystallisations from the mother liquor produced the tetranitrate complex as green crystals. The tetranitrate was recrystallised from water and vacuum dried (80°, 0.05 mm Hg for 3 hrs).

YIELD:  $[\text{PAP}_2\text{Ni}_2(\text{OH})(\text{NO}_3)_3]$  0.37 g

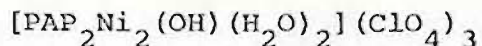
ANALYSES  $[\text{PAP}_2\text{Ni}_2(\text{OH})(\text{NO}_3)_3]$  FOUND C 45.69% H 3.44% N 22.24%

REQ. C 45.56% H 3.08% N 22.14%

YIELD:  $[\text{PAP}_2\text{Ni}_2(\text{NO}_3)_4]$  0.54 g

ANALYSES  $[\text{PAP}_2\text{Ni}_2(\text{NO}_3)_4]$  FOUND C 43.46% H 2.81% N 22.53% Ni 11.80%

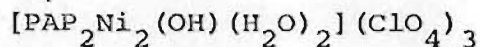
REQ. C 43.49% H 2.84% N 22.54% Ni 11.81%



The preparative procedure for this complex is the same as that described for  $[\text{PAP}_2\text{Ni}_2(\text{H}_2\text{O})_4]\text{Cl}_4 \cdot n\text{H}_2\text{O}$ , using 1.50 g PAP (4.77 mmoles) and an excess of nickel perchlorate. As the complex is not very soluble, the reaction was carried out in 600 ml. water to ensure all of the complex formed would be in solution. The product was obtained as green crystals. The product was recrystallised from water and dried under vacuum (80°, 0.05 mm Hg for 3 hours).

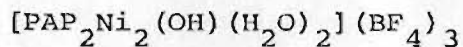
YIELD: 1.23 g (47%)

ANALYSES



FOUND C 39.80% H 2.71% N 15.50% Ni 10.91%

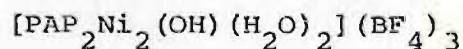
REQ. C 39.40% H 3.03% N 15.31% Ni 10.70%



The reaction procedure was the same as that for the preparation of the perchlorate complex, using 1.50 g PAP (4.77 mmoles) and excess nickel tetrafluoroborate. This compound also formed green crystals. The product was recrystallised from water and dried in vacuum for 3 hours at 80° and 0.05 mm Hg.

YIELD: 1.14 g (45%)

ANALYSES



FOUND C 40.44% H 3.13% N 15.72% Ni 10.40%

REQ. C 40.77% H 3.23% N 15.85% Ni 11.07%

ZINC COMPLEXES

The procedure for the preparation of the PAP-Zinc complexes was the same in all cases. A slight excess of the zinc salt (>1:1 metal:ligand ratio) was dissolved in 20 ml methanol and the solution filtered. To this solution was added a solution of 0.5 g PAP dissolved in boiling methanol. Within a few minutes the complex came out of solution as a cream or yellow amorphous precipitate. The insolubility of these complexes in common laboratory solvents did not allow purification by recrystallisation. Yields were between 75%-80%. The results of the elemental analyses of the zinc complexes are shown in Table 13.

TABLE 13  
ELEMENTAL ANALYSES OF PAP-Zn COMPLEXES

COMPOUND	FOUND				REQUIRED			
	%C	%H	%N	%Zn	%C	%H	%N	%Zn
$[\text{PAP}_2\text{Zn}_2\text{Cl}_4]$	48.8	3.09	18.4	14.4	48.2	3.12	18.7	14.5
$[\text{PAPZnBr}_2] \cdot \text{H}_2\text{O}$	37.6	2.48	14.6	12.5	37.6	3.15	14.6	11.4
$[\text{PAPZnI}_2] \cdot \text{H}_2\text{O}$	33.5	2.22	12.8	10.3	33.2	2.47	12.9	10.0
$[\text{PAP}_2\text{Zn}_2(\text{SCN})_4] \cdot \text{H}_2\text{O}$	47.0	2.94	20.7	-	46.7	3.11	21.8	-

REFERENCES

1. A.B.P. Lever; Ph.D. Thesis (1959). Imperial College, London.
2. L.K. Thompson; Ph.D. Thesis (1968), University of Manchester, Institute of Science and Technology.
3. A.R. Katritzky, A.R. Hands; J. Chem. Soc., 2202 (1958).
4. D.A. Baldwin, A.B.P. Lever, R.V. Parish; Inorg. Chem., 8, 107 (1969).
5. S.P. Sinha; Spectrochim. Acta., 20, 879 (1964).
6. P.E. Figgins, D.H. Busch; J. Phys. Chem., 65, 2236 (1961).
7. L.K. Thompson, V.T. Chacko, J.A. Elvidge, A.B.P. Lever, R.V. Parish; Can. J. Chem., 47, 4141 (1969).
8. A.B.P. Lever, L.K. Thompson, W.M. Reiff; Inorg. Chem., 11, 104 (1972).
9. E.C. Lingafelter; Private communication to A.B.P. Lever.
10. M.S. Haddad, D.N. Henrickson; Inorg. Chim. Acta., 28 (1978) L121.
11. L.K. Thompson; Unpublished observations.
12. W.J. Stratton, D.H. Busch; J. Am. Chem. Soc., 78, 1137 (1956).
13. W.J. Stratton, D.H. Busch; *ibid.*, 80, 1286 (1958).
14. W.J. Stratton, D.H. Busch; *ibid.*, 82, 4833 (1960).
15. P.W. Ball, A.B. Blake; J. Chem. Soc., (A), 1415 (1969).
16. P.W. Ball, A.B. Blake; J.C.S. Dalton, 852 (1974).
17. J.E. Andrew, A.B. Blake; J. Chem. Soc., (A), 1408 (1969).
18. W. Rosen; Inorg. Chem., 10, 1832 (1971).
19. E.K. Barefield, D.H. Busch, S.M. Nelson; Quart. Rev. Chem. Soc., 22, 457 (1968).
20. D.A. Sullivan, G.J. Palenik; Inorg. Chem., 16, 1127 (1977).

21. C.J. Ballhausen; Introduction to Ligand Field Theory, McGraw-Hill, New York (1962).
22. A. Ludi, W. Feitknecht; *Helv. Chim. Acta.*, 46, 2226 (1963).
23. C.K. Jorgensen; *Acta. Chem. Scand.*, 9, 1362 (1955).
24. O.G. Holmes, D.S. McClure; *J. Chem. Phys.*, 26, 1686 (1957).
25. A.D. Liehr, C.J. Ballhausen; *Ann. Phys.*, 6, 134 (1959),  
*Mol. Phys.*, 2, 123 (1959).
26. C. Furlani; *Gazz. Chim. Ital.*, 88, 279 (1958).
27. N.C. Stephenson; *Acta. Cryst.*, 17, 592 (1964).
28. J.C. Bailar (ed.); Comprehensive Inorganic Chemistry, Vol. III  
p 1156, Pergamon Press, Oxford, 1973.
29. S. Mizushima, J.V. Quagliano; *J. Am. Chem. Soc.*, 75, 4870 (1953).
30. N.F. Curtis, J.M. Curtis; *Inorg. Chem.*, 4, 804 (1965).
31. A.B.P. Lever, E. Mantovani, B.S. Ramaswamy; *Can. J. Chem.*,  
49, 1957 (1971).
32. K. Nakamoto; Infrared Spectra of Inorganic and Coordination  
Compounds, John Wiley and Sons, New York, N.Y. 1963.
33. D. Scargill; *J. Chem. Soc.*, 4440 (1961).
34. F.A. Miller, C.H. Wilkins; *Analyt. Chem.*, 24, 1253 (1952).
35. B.J. Hathaway, A.E. Underhill; *J. Chem. Soc.*, 3091 (1961).
36. N.N. Greenwood; *J. Chem. Soc.*, 3811 (1959).
37. F.A. Cotton, G. Wilkinson; Advanced Inorganic Chemistry, 3rd  
edition, p 233, Interscience Publishers, New York 1972.
38. J.R. Allan, G.A. Barnes, D.H. Brown; *J. Inorg. Nucl. Chem.*,  
33, 3765 (1971).
39. H.C. Clark, R.J. O'Brien; *Can. J. Chem.*, 39, 1030 (1961).

### Appendix A

The temperature dependent magnetic susceptibility studies were determined by the Gouy method on equipment in the Chemistry Department at the University of British Columbia (refer to page 67). The molar susceptibilities were corrected for temperature independent paramagnetism ( $TIP = 8N\beta^2/(10 Dq) = 2.08/(10 Dq)$  c.g.s. units), and also for diamagnetic effects of ligand, etc. as mentioned in description of magnetic susceptibility studies. The susceptibility of a pair of atoms in a spin triplet, orbital singlet state is given by:

$$\chi_M^{CORR} = \frac{2N\beta^2 g^2}{kT} \left( \frac{e^{-4x} + 5}{e^{-6x} + 3e^{-4x} + 5} \right)$$

$$x = J/kT$$

The values of  $g$  and  $J$  were determined using a linear regression of the form  $y = m\hat{x} + b$  where  $y$  is the experimental value of  $\chi_M^{CORR}$ ,  $m = 2N\beta^2 g^2$  and  $\hat{x}$  is a function of  $T$ ,

$$\text{i.e.} \quad \hat{x} = \frac{1}{kT} \left( \frac{e^{-4x} + 5}{e^{-6x} + 3e^{-4x} + 5} \right)$$

An iterative procedure was used until a value of  $J$  was found that gave  $b = 0$ . The corresponding slope  $m$  for this  $\hat{x}$  was used to determine the value of  $g$ . The computer program used to determine  $g$  and  $J$  is given at the end of this appendix.



TABLE A-1

MAGNETIC SUSCEPTIBILITIES (CORRECTED FOR TIP AND DIAMAGNETISM)

(c.g.s. units per formula weight)

COMPLEX	T	$10^6 \chi_M^{CORR}$
$[\text{PAP}_2\text{Ni}_2(\text{H}_2\text{O})_4]\text{Cl}_4 \cdot 3\text{H}_2\text{O}$	302.2	7809.95
$g = 2.16$	277.2	8546.91
$J = 3.16 \text{ cm}^{-1}$	256.0	9358.03
	235.8	10229.4
	214.0	11295.5
	191.5	12611.8
$[\text{PAP}_2\text{Ni}_2(\text{OH})(\text{H}_2\text{O})_2](\text{ClO}_4)_3$	260.5	7132.2
	245.5	7529.4
$g = 1.93$	227.0	8126.4
$J = -7.31 \text{ cm}^{-1}$	207.0	8783.8
	187.0	9557.6
	167.0	10601
	145.5	11947

```

0001      IMPLICIT REAL * 8 (A-H,O-Z)
0002      DIMENSION AT(20), AX(20), X(20), Y(20), P(50,10), C(10), S(10), A(10), R(1
X(1), T(10,10), V(10), SC(2), W(20), CY(20), SDIF(20), BX(20), Z(20)
0003      N = 0
0004      1 N = N + 1
0005      READ (5,2) AT(N), AX(N), RSO
0006      2 FORMAT (6X,D10.3,2X,D11.4,2X,FS,1)
0007      IF (RSO) 1,1,3
0008      3 AJ = 0.00
0009      4 AINC = 0.01
0010      AJ = AJ + AINC
0011      IF (AJ .LT. -10.00) GO TO 7
0012      I = 0
0013      5 I = I + 1
0014      Y(I) = AX(I)
0015      BX(I) = AJ / (AT(I) * 0.69503)
0016      X(I) = (BX(I) * (DEXP(-4.0 * BX(I)) + 5.0)) / (AJ * (DEXP(-6.0 * B
XY(I)) + (3.0 * (DEXP(-4.0 * BX(I))) + 5.0))
0017      Z(I) = X(I)
0018      IF (I .LT. N) GO TO 5
0019      MD = 1
0020      CALL RLFOTH (X, Y, N, RSO, MD, ID, P, C, S, A, B, IER)
0021      CALL RLDOPI (C, ID, A, B, f)
0022      SSE = 3(ID+3)
0023      IOPT = 0
0024      IP = 50
0025      CALL RLDCW (SSE, X, W, N, ID, IOPT, A, B, V, P, IP, IER)
0026      SC(1) = C(ID+2)
0027      SC(2) = C(ID+3)
0028      IT = 10
0029      CALL RLDCVA (V, ID, A, B, SC, T, IT, IER)
0030      G = DSQRT(C(2) / 0.26074)
0031      PEG = 0.6745 * DSQRT(V(2)) * G / C(2)
0032      PPEG = DABS(100.0 * PEG / G)
0033      R = 0.0
0034      SSD = 0.0
0035      DO 10 I=1, N
0036      CY(I) = (C(2) * Z(I)) + C(1)
0037      SDIF(I) = (Y(I) - CY(I)) ** 2
0038      SSD = SSD + SDIF(I)
0039      R = (SDIF(I) / (Y(I) ** 2)) + R
0040      10 CONTINUE
0041      R = DSQRT(R)
0042      WRITE (6,6) C(1), C(2), AJ, G, PPEG, SSD, R
0043      6 FORMAT ('0', 2X, 7(D14.7, 2X))
0044      GO TO 4
0045      7 CONTINUE
0046      WRITE (6,20)

```

0047  
0048  
0049

20 FORMAT ('0',38H THIS IS THE LAST J VALUE IN THE RANGE)  
STOP  
END





